patients with NASH, impaired glutathione metabolism and antioxidant enzyme activity probably cause an increase in oxidative stress.[42]

The Ath diet induces an Ath lipid profile, including an increase in small dense LDL-C, which is highly susceptible to oxidation, and then leads to oxidized low-density lipoprotein (LDL), which induces an inflammatory response in endothelial cells.[43] In the livers of mice fed the Ath diet, the expression levels of genes for CD36 antigen and scavenger receptor type B member 1, which are receptors for oxidized LDL,[44] tended to be up-regulated (Supplementary Table 2). Therefore, it might be possible that up-regulated receptors for oxidized LDL enhance the uptake of increasing levels of small dense LDL-C and contribute to inflammation in the liver.

In response to the lipid-induced oxidative stress, genes involved in fibrogenesis were coordinately up-regulated. Indeed, the hepatic expression of TNF-α and NADPH oxidase complex genes preceded that of fibrogenic genes, and this suggested that inflammation precedes the fibrogenic process in our models. The expression of TGF-β and PAI-1 genes was up-regulated dramatically, especially in the Ath+HF group. PAI-1 is a key factor in matrix remodeling, and the gene is highly induced in response to TGF-β.[45] Urokinase plasminogen activator generates plasmin, and this process is inhibited by PAI-1. Plasmin degrades the extracellular matrix both directly and by activating matrix metalloproteinases.[46] Therefore, PAI-1 inhibits collagenolysis by inhibiting the generation of plasmin in the liver. Consequently, the inhibition of collagenolysis, in addition to the overall up-regulation of collagen genes, might contribute to hepatic fibrosis in this model.

In summary, we report that the Ath diet induces steatohepatitis with cellular ballooning via cholesterol-induced oxidative stress and hepatic insulin resistance. Adding a high-fat component further aggravates oxidative stress and steatohepatitis, possibly by inducing insulin resistance and down-regulating genes for antioxidant enzymes. This model suggests the critical and different roles of cholesterol, TG, and FFAs in causing oxidative stress and insulin resistance leading to steatohepatitis and provides a system for screening therapeutic targets to treat NASH and atherosclerosis.

Acknowledgment: We thank Dr. Isao Usui, Dr. Hajime Ishihara, and Professor Toshiyasu Sasaoka of Toyama University for their technical advice concerning western blot analyses.

References

1. Marchesini G, Bugianesi E, Forlani G, Cerrelli F, Lenzi M, Manini R, et al. Nonalcoholic fatty liver, steatohepatitis, and the metabolic syndrome. HEPATOLOGY 2003;37:917-923.
2. Sanyal AJ. AGA technical review on nonalcoholic fatty liver disease. Gastroenterology 2002;123:1705-1725.
3. James OF, Day CP. Non-alcoholic steatohepatitis (NASH): a disease of emerging identity and importance. J Hepatol 1998;29:495-501.
4. Targher G, Bertolini L, Poli F, Rodella S, Scala L, Tessari R, et al. Nonalcoholic fatty liver disease and risk of future cardiovascular events among type 2 diabetic patients. Diabetes 2005;54:3541-3546.
5. Chen H, Charlat O, Tartaglia LA, Woolf EA, Weng X, Ellis SJ, et al. Evidence that the diabetes gene encodes the leptin receptor: identification of a mutation in the leptin receptor gene in db/db mice. Cell 1996;84:491-495.
6. Shimano H, Horton JD, Hammer RE, Shimomura I, Brown MS, Goldstein JL. Overproduction of cholesterol and fatty acids causes massive liver enlargement in transgenic mice expressing truncated SREBP-1a. J Clin Invest 1996;98:1575-1584.
7. Surwit RS, Feinglos MN, Rodin J, Sutherland A, Petro AE, Opara EC, et al. Differential effects of fat and sucrose on the development of obesity and diabetes in C57BL/6J and A/J mice. Metabolism 1995;44:645-651.
8. Weltman MD, Farrell GC, Liddle C. Increased hepatocyte CYP2E1 expression in a rat nutritional model of hepatic steatosis with inflammation. Gastroenterology 1996;111:1645-1653.
9. Leclercq IA, Farrell GC, Field J, Bell DR, Gonzalez FJ, Robertson GR. CYP2E1 and CYP4A as microsomal catalysts of lipid peroxides in murine nonalcoholic steatohepatitis. J Clin Invest 2000;105:1067-1075.
10. Rinella ME, Green RM. The methionine-choline deficient dietary model of steatohepatitis does not exhibit insulin resistance. J Hepatol 2004;40:47-51.
11. Ota T, Takamura T, Kurita S, Matsuzawa N, Kita Y, Uno M, et al. Insulin resistance accelerates a dietary rat model of nonalcoholic steatohepatitis. Gastroenterology 2007;132:282-293.
12. Paigen B, Morrow A, Brandon C, Mitchell D, Holmes P. Variation in susceptibility to atherosclerosis among inbred strains of mice. Atherosclerosis 1985;57:65-73.
13. Jeong WI, Jeong DH, Do SH, Kim YK, Park HY, Kwon OD, et al. Mild hepatic fibrosis in cholesterol and sodium cholate diet-fed rats. J Vet Med Sci 2005;67:235-242.
14. Usui S, Hara Y, Hosaki S, Okazaki M. A new on-line dual enzymatic method for simultaneous quantification of cholesterol and triglycerides in lipoproteins by HPLC. J Lipid Res 2002;43:805-814.
15. Miyake K, Ogawa W, Matsumoto M, Nakamura T, Sakaue H, Kasuga M. Hyperinsulinemia, glucose intolerance, and dyslipidemia induced by acute inhibition of phosphoinositide 3-kinase signaling in the liver. J Clin Invest 2002;110:1483-1491.
16. Yamauchi T, Nio Y, Maki T, Kobayashi M, Takazawa T, Iwabu M, et al. Targeted disruption of AdipoR1 and AdipoR2 causes abrogation of adiponectin binding and metabolic actions. Nat Med 2007;13:332-339.
17. Brunt EM, Janney CG, Di Bisceglie AM, Neuschwander-Tetri BA, Bacon BR. Nonalcoholic steatohepatitis: a proposal for grading and staging the histological lesions. Am J Gastroenterol 1999;94:2467-2474.
18. Folch J, Lees M, Sloane Stanley GH. A simple method for the isolation and purification of total lipides from animal tissues. J Biol Chem 1957;226:497-509.
19. Bataller R, Schwabe RF, Choi YH, Yang L, Paik YH, Lindquist J, et al. NADPH oxidase signal transduces angiotensin II in hepatic stellate cells and is critical in hepatic fibrosis. J Clin Invest 2003;112:1383-1394.
20. Doniger SW, Salomonis N, Dahlquist KD, Vranizan K, Lawlor SC, Conklin BR. MAPPFinder: using Gene Ontology and GenMAPP to create a global gene-expression profile from microarray data. Genome Biol 2003;4:R7.
21. Dahlquist KD, Salomonis N, Vranizan K, Lawlor SC, Conklin BR. GenMAPP, a new tool for viewing and analyzing microarray data on biological pathways. Nat Genet 2002;31:19-20.
22. Matloff DS, Selinger MJ, Kaplan MM. Hepatic transaminase activity in alcoholic liver disease. Gastroenterology 1980;78:1389-1392.
23. Friedman SL. Molecular regulation of hepatic fibrosis, an integrated cellular response to tissue injury. J Biol Chem 2000;275:2247-2250.

24. Leonarduzzi G, Scavazza A, Biasi F, Chiarpotto E, Camandola S, Vogel S, et al. The lipid peroxidation end product 4-hydroxy-2,3-nonenal up-regulates transforming growth factor beta1 expression in the macrophage lineage: a link between oxidative injury and fibrosclerosis. FASEB J 1997; 11:851-857.
25. Shimano H, Yahagi N, Amemiya-Kudo M, Hasty AH, Osuga J, Tamura Y, et al. Sterol regulatory element-binding protein-1 as a key transcription factor for nutritional induction of lipogenic enzyme genes. J Biol Chem 1999;274:35832-35839.
26. Aoyama T, Peters JM, Iritani N, Nakajima T, Furihata K, Hashimoto T, et al. Altered constitutive expression of fatty acid-metabolizing enzymes in mice lacking the peroxisome proliferator-activated receptor alpha (PPARalpha). J Biol Chem 1998;273:5678-5684.
27. Sanyal AJ, Campbell-Sargent C, Mirshahi F, Rizzo WB, Contos MJ, Sterling RK, et al. Nonalcoholic steatohepatitis: association of insulin resistance and mitochondrial abnormalities. Gastroenterology 2001;120: 1183-1192.
28. Chalasani N, Gorski JC, Asghar MS, Asghar A, Foresman B, Hall SD, et al. Hepatic cytochrome P450 2E1 activity in nondiabetic patients with nonalcoholic steatohepatitis. HEPATOLOGY 2003;37:544-550.
29. Li Z, Yang S, Lin H, Huang J, Watkins PA, Moser AB, et al. Probiotics and antibodies to TNF inhibit inflammatory activity and improve nonalcoholic fatty liver disease. HEPATOLOGY 2003;37:343-350.
30. Day CP, James OF. Steatohepatitis: a tale of two "hits"? Gastroenterology 1998;114:842-845.
31. De Minicis S, Bataller R, Brenner DA. NADPH oxidase in the liver: defensive, offensive, or fibrogenic? Gastroenterology 2006;131:272-275.
32. Vergnes L, Phan J, Strauss M, Tafuri S, Reue K. Cholesterol and cholate components of an atherogenic diet induce distinct stages of hepatic inflammatory gene expression. J Biol Chem 2003;278:42774-42784.
33. Liao F, Andalibi A, de Beer FC, Fogelman AM, Lusis AJ. Genetic control of inflammatory gene induction and NF-kappa B-like transcription factor activation in response to an atherogenic diet in mice. J Clin Invest 1993; 91:2572-2579.
34. Ginsberg HN. Is the slippery slope from steatosis to steatohepatitis paved with triglyceride or cholesterol? Cell Metab 2006;4:179-181.
35. Mari M, Caballero F, Colell A, Morales A, Caballeria J, Fernandez A, et al. Mitochondrial free cholesterol loading sensitizes to TNF- and Fas-mediated steatohepatitis. Cell Metab 2006;4:185-198.
36. Kleiner DE, Brunt EM, Van Natta M, Behling C, Contos MJ, Cummings OW, et al. Design and validation of a histological scoring system for nonalcoholic fatty liver disease. HEPATOLOGY 2005;41:1313-1321.
37. Kim JK, Fillmore JJ, Chen Y, Yu C, Moore IK, Pypaert M, et al. Tissue-specific overexpression of lipoprotein lipase causes tissue-specific insulin resistance. Proc Natl Acad Sci U S A 2001;98:7522-7527.
38. Horton JD, Shimomura I, Brown MS, Hammer RE, Goldstein JL, Shimano H. Activation of cholesterol synthesis in preference to fatty acid synthesis in liver and adipose tissue of transgenic mice overproducing sterol regulatory element-binding protein-2. J Clin Invest 1998;101:2331-2339.
39. Ide T, Shimano H, Yahagi N, Matsuzaka T, Nakakuki M, Yamamoto T, et al. SREBPs suppress IRS-2-mediated insulin signalling in the liver. Nat Cell Biol 2004;6:351-357.
40. Nakagawa Y, Shimano H, Yoshikawa T, Ide T, Tamura M, Furusawa M, et al. TFE3 transcriptionally activates hepatic IRS-2, participates in insulin signaling and ameliorates diabetes. Nat Med 2006;12:107-113.
41. Miyazaki M, Dobrzyn A, Sampath H, Lee SH, Man WC, Chu K, et al. Reduced adiposity and liver steatosis by stearoyl-CoA desaturase deficiency are independent of peroxisome proliferator-activated receptor-alpha. J Biol Chem 2004;279:35017-35024.
42. Nobili V, Pastore A, Gaeta LM, Tozzi G, Comparcola D, Sartorelli MR, et al. Glutathione metabolism and antioxidant enzymes in patients affected by nonalcoholic steatohepatitis. Clin Chim Acta 2005;355:105-111.
43. Galeano NF, Al-Haideri M, Keyserman F, Rumsey SC, Deckelbaum RJ. Small dense low density lipoprotein has increased affinity for LDL receptor-independent cell surface binding sites: a potential mechanism for increased atherogenicity. J Lipid Res 1998;39:1263-1273.
44. Endemann G, Stanton LW, Madden KS, Bryant CM, White RT, Protter AA. CD36 is a receptor for oxidized low density lipoprotein. J Biol Chem 1993;268:11811-11816.
45. Chapman HA. Disorders of lung matrix remodeling. J Clin Invest 2004; 113:148-157.
46. Leyland H, Gentry J, Arthur MJ, Benyon RC. The plasminogen-activating system in hepatic stellate cells. HEPATOLOGY 1996;24:1172-1178.

Hepatitis B virus X protein overcomes oncogenic RAS-induced senescence in human immortalized cells

Naoki Oishi,[1,2] Khurts Shilagardi,[1] Yasunari Nakamoto,[2] Masao Honda,[2] Shuichi Kaneko[2] and Seishi Murakami[1,3]

[1]Department of Signal Transduction, Cancer Research Institute; [2]Department of Disease Control and Homeostasis, Graduate School of Medicine, Kanazawa University, 13-1 Takara-machi, Kanazawa 920-0934, Japan

(Received February 23, 2007/Revised June 12, 2007/Accepted June 25, 2007/Online publication August 19, 2007)

Chronic infection with hepatitis B virus (HBV) is a major risk factor for hepatocellular carcinoma. The HBV X protein (HBx) is thought to have oncogenic potential, although the molecular mechanism remains obscure. Pathological roles of HBx in the carcinogenic process have been examined using rodent systems and no report is available on the oncogenic roles of HBx in human cells *in vitro*. We therefore examined the effect of HBx on immortalization and transformation in human primary cells. We found that HBx could overcome active RAS-induced senescence in human immortalized cells and that these cells could form colonies in soft agar and tumors in nude mice. HBx alone, however, could contribute to neither immortalization nor transformation of these cells. In a population doubling analysis, an N-terminal truncated mutant of HBx, HBx-D1 (amino acids 51–154), which harbors the coactivation domain, could overcome active RAS-induced cellular senescence, but these cells failed to exhibit colonigenic and tumorigenic abilities, probably due to the low expression level of the protein. By scanning a HBx expression library of the clustered-alanine substitution mutants, the N-terminal domain was found to be critical for overcoming active RAS-induced senescence by stabilizing full-length HBx. These results strongly suggest that HBx can contribute to carcinogenesis by overcoming active oncogene-induced senescence. (*Cancer Sci* 2007; 98: 1540–1548)

Chronic infection with HBV is a major risk factor for HCC worldwide. HBV belongs to the Hepadnavirus family. Its genome is a 3.2-kb, circular, partially double-stranded DNA molecule with four overlapping open reading frames: PC-C, PS-S, P and X.[1] The HBV genome, which is converted to covalently closed circular DNA in the nucleus after infection, serves as the template for transcription, generating the four viral transcripts that encode the HBV core and polymerase polypeptides, the large surface antigen polypeptide, the middle and major surface antigen polypeptides, and the HBx polypeptide. HBV replicates by reverse transcription of viral pregenomic 3.5-kb RNA using the HBV polymerase that catalyzes RNA-dependent DNA synthesis and DNA-dependent DNA synthesis.[1,2] It is converted into the 3.2-kb partially double-stranded genomic DNA inside the viral capsid.

The critical role of HBV chronic infection in HCC has been well established etiologically, whereas the mechanism by which HBV causes transformation of hepatocytes remains unclear.[3–5] HBx has long been suspected of playing a positive role in hepatocarcinogenesis, as avian hepadnaviruses missing the X open reading frame seem not to be associated with HCC. HBx consists of 154 aa and is a multifunctional regulator that modulates many host cell functions through its interactions with a variety of host factors.[5] HBx consists of both a negative regulatory domain[6] and a coactivation domain that is required for the augmentation of virus and host genes.[7,8] HBx was reported to transform rodent immortal cells *in vitro*,[9,10] and a high incidence of HCC has been reported in transgenic mice overexpressing HBx.[11,12] However, the functional role of HBx in the transformation is still controversial. Some independent groups proposed collaborating roles of HBx in the hepatocarcinogenic process.[13–15] Although these reports are informative, all were experimentally assessed in rodent systems. Because mouse and human primary cells have different telomere biology,[16] DNA damage check point control mechanisms and cell cycle progression,[17,18] developing a human system to address the functional role of HBx is critically important. Here we report that we established human fibroblast cells stably expressing HBx protein and analyzed the effects of HBx expression on the ability to confer an immortal phenotype and tumorigenic potential.

Materials and Methods

Retroviral vectors. All constructs for the expression of HBx (subtype adr) proteins, pNKF-HBx (aa 1–154), pNKF-HBx-D1 (aa 1–50) and pNKF-HBx-D5 (aa 51–154) have been described previously.[8] The retrovirus vectors pBabe-puro, hygro, puro-H-RAS^{V12} hygro-hTERT and pWZL-blast were kindly provided by W. C. Hahn (Dana-Farber Cancer Institute, Harvard).[19,20] To construct pBabe-blast, the blasticidin S cDNA of pWZL-blast was used as a template to amplify the PCR products of blasticidin S with the primer set of AAGCTTACCATGGCCAAGCCTTTGT and ATCGATTTAGCCCTCCCACACATAA, generating an artificial *Hind*III site at the 5-end and a *Cla*I site at the 3′-end, respectively. The HBx cDNA of pNKF-HBx was used as a template to amplify the PCR products of HBx with a primer set of TGATCAATGGACTACAAAGACGAT and CTCGAGAGATCTTTAATTAATTAA, generating an artificial *Fba*I site at the 5-end and an *Xho*I site at the 3′-end, respectively. The PCR products were digested and inserted into the *Bam*HI and *Sal*I sites of the pBabe-blast vector. The *Eco*RI and *Bgl*II fragments of HBx-D1 and HBx-D5 from pNKF-HBx-D1 and pNKF-HBx-D5 were, respectively, inserted into the *Eco*RI and *Bgl*II sites of the pBabe-blast-HBx vectors. An alanine scanning method was applied to construct a series of HBx clustered alanine substitution mutants (designated 'cm') by site-directed mutagenesis. The mutagenesis was carried out using a splicing PCR method with all of the mutated oligonucleotide primer sets. The target sequence of seven aa residues was changed to AAASAAA, and all of the HBx-encoding DNA fragments bearing the clustered mutations were introduced into the *Eco*RI and *Bam*HI sites of pNKFLAG, generating the pNKF-Xcm1 to pNKF-Xcm21 constructs. The

[3]To whom correspondence should be addressed.
E-mail: semuraka@kenroku.kanazawa-u.ac.jp

Abbreviations: aa, amino acid; DMEM, Dulbecco's modified Eagle's medium; HBV, hepatitis B virus; HBx, hepatitis B virus X protein; HCC, hepatocellular carcinoma; hTERT, human telomerase reverse transcriptase; OIS, oncogene-induced senescence; PCR, polymerase chain reaction; PD, population doubling; SA-β-gal, senescence-associated β-galactosidase; SDS-PAGE, sodium dodecylsulfate–polyacrylamide gel electrophoresis.

doi: 10.1111/j.1349-7006.2007.00579.x

*Eco*RI and *Bgl*II fragments of HBx-cm1 to HBx-cm21 from pNKF-Xcm1 to pNKF-Xcm21 were, respectively, inserted into the *Eco*RI and *Bgl*II sites of the pBabe-blast-HBx vectors. All of the constructs were sequenced by the dideoxy method using the *Taq* sequencing primer kit and a DNA sequencer (370A; Applied Biosystems).

Virus production and cell lines. Amphotropic retroviruses were produced by transfection of the 293T producer cell line with a retroviral vector and a vector encoding replication-defective helper viruses, pCL-Ampho (Imgenex), using FuGENE 6 transfection reagent (Roche Applied Science) according to the manufacturer's recommendations. Two days after the transfection, culture supernatants were collected, filtered, supplemented with 4 μg/mL polybrene, and used for infection. Two days after the infection, drug selection of infected cells was started, and the selected populations were used in all of the experiments. Infected cell populations were selected in puromycin (1.0 μg/mL), blasticidin S (4 μg/mL) and hygromycin (80 μg/mL) for up to 2 weeks.

Cell culture. Human lung fibroblasts (TIG3) from the Japanese Collection of Research Bioresources were maintained in DMEM with 10% heat-inactivated fetal bovine serum (JRH Biosciences). Human foreskin fibroblasts, BJ and BJ-hTERT-LT-ST-H-RAS^{V12} cells were maintained as described previously.[19] These human fibroblasts were not clonal and were maintained as populations. BJ cells and TIG3 cells have a finite lifespan, and were used at PD between 25 and 35. PD were determined using the formula:

$$PD = Log(Nf/Ni)/Log2,$$

where Nf = the number of cells counted and Ni = the number of cells seeded. Comparisons of means and standard deviations were carried out using the unpaired *t*-test.

Western blot analysis. Cells were harvested, washed with phosphate-buffered saline (–), and sonicated in a lysis buffer (50 mM Tris-HCl [pH 7.4], 200 mM NaCl, 1 mM ethylenediaminetetraacetic acid, 10% glycerol, 1 mM phenylmethylsulfonyl fluoride, 10 μg/mL leupeptin, 10 μg/mL aprotinin and 10 μg/mL dithiothreitol). Total lysates were fractionated by SDS-PAGE, transferred onto nitrocellulose membranes and subjected to western blot analysis with antibodies. Anti-FLAG M2 antibody and anti-β-actin antibody were from Sigma. Anti-RAS antibody F-235 (sc-29), anti-p53 antibody DO-1 (sc-126) and anti-p21 antibody F-5 (sc-6246) were from Santa Cruz. Anti-p16 antibody was from BD PharMingen. The proteins were visualized by enhanced chemiluminescence according to the manufacturer's instructions (Amersham).

Analysis of senescence. SA-β-Gal staining was carried out using the Senescence Detection Kit (Oncogene) as instructed by the manufacturer. For each sample, at least 200 cells were counted in randomly chosen fields.

Telomerase activity assays. Total lysates of cells were subjected to the telomerase repeat amplification protocol using a TRAPEZE kit (Intergen) according to the manufacturer's instructions.

Soft-agar colony formation assays. Soft-agar growth assays were carried out as described previously.[19] At the time of plating in soft agar, cultures were trypsinized and counted, and 5×10^3 or 5×10^4 total cells were mixed with 1.5 mL of 0.35% Noble agar-DMEM (top layer) and then poured on top of 5 mL of solidified 0.7% Noble agar-DMEM (bottom layer) in 6-cm-diameter dishes. After 3 weeks, colonies were counted, and pictures were taken.

Tumorigenicity assays. A total of 1×10^6 cells were resuspended in 50 μL Matrigel solution (BD Matrigel Basement Membrane Matrix HC; BD Biosciences) and immediately injected subcutaneously into 8-week-old female nude mice (BALB/cAnNCrl-nu BR). 2-D tumor sizes were measured once a week. The tumor volume (mm^3) was calculated using the formula (length × width^2)/2.[21]

Results

Effect of HBx on cellular senescence of human primary cells. During immortalization, human cells differ from rodent cells in the regulation of telomere length[22,23] and cell cycle checkpoints.[24,25] Human cells must bypass two barriers to become immortalized: replicative senescence and crisis. Replicative senescence is characterized by an irreversible growth arrest but continued metabolic activity.[26] Crisis is characterized by widespread cell death.[26,27] By the introduction of hTERT, human primary cells avoid these two barriers and can become immortalized.[28–30]

It is possible that HBx contributes to the immortalization process of human primary cells, but not to the cellular transformation process. If so, it may facilitate cellular transformation indirectly by overcoming two crises, M1 and M2. To study whether this does facilitate cellular transformation, it is best to use human primary hepatocytes as HBV is a hepatotropic virus. However, human primary hepatocytes are almost impossible to obtain for such an experimental approach. HBx exhibits its transactivation function not only in hepatoma cell lines but also in various carcinoma and sarcoma cell lines. Under these situations, we addressed whether HBx contributes to the immortalization of human primary fibroblasts, BJ cells and TIG3 cells that have been well studied for cellular senescence and immortalization. We used hTERT-introduced BJ and TIG3 cells for positive controls of immortal cells.

The human primary fibroblasts, BJ cells and TIG3 cells were infected with the HBx-expression retroviruses and cultured in the presence of the selection drug, blasticidin S. The drug-resistant polyclonal cells were selected and characterized. Three different constructs of HBx were used to map the responsible domain: full-length HBx (HBx-wt), HBx-D1, which lacks the N-terminal negative regulatory domain, and HBx-D5, which lacks the coactivation domain (Fig. 1a). First we examined HBx expression in the primary human fibroblasts. We found that full-length HBx and HBx-D5 were highly but equally expressed, whereas expression of HBx-D1 was very weak in the blastcidin S-selected clones (Fig. 1b). We hypothesized that HBx expression may confer an immortal phenotype, which could contribute to cellular transformation and tumorigenesis, but we observed that the BJ cells expressing HBx proteins stopped dividing at PD 69.6 ± 0.9 (errors ± SD) (HBx-wt), PD 66.6 ± 1.6 (HBx-D5), PD 66.1 ± 1.4 (HBx-D1) and PD 60.5 ± 0.6 (control cells) (Fig. 1c). TIG3 cells, another human fibroblast, expressing HBx proteins stopped dividing at PD 77.2 ± 1.1 (HBx-wt), PD 75.1 ± 0.8 (HBx-D5), PD 75.1 ± 0.1 (HBx-D1) and PD 75.4 ± 0.2 (control cells) (Fig. 1d). Although a very minor extended lifespan (2–4 PD) was observed with HBx-wt-expressing primary human fibroblasts, the HBx protein could not elicit immortalization. We examined whether the effect of HBx on delay of cellular senescence was correlated with putative augmentation of telomerase activity in HBx-introduced BJ and TIG3 cells (Fig. 1e) as activation of the hTERT promoter was observed in hepatoma cell lines that were transiently cotransfected with the HBx expression vector and luciferase reporter vector of the hTERT promoter (S. Murakami *et al.* unpublished data, 2005). Telomerase activity in the extracts of cells expressing HBx-wt or HBx-D1 was slightly higher than that of cells expressing empty vector or HBx-D5 in both kinds of cells (Fig. 1e), but we failed to detect an increase in hTERT protein expression (data not shown). Therefore, the relevance of the weak augmentation of telomerase activity in the HBx-expressing primary cells remains unclear.

Effect of HBx on immortalized BJ-hTERT cells. Next, we addressed whether HBx facilitates the cellular transformation process

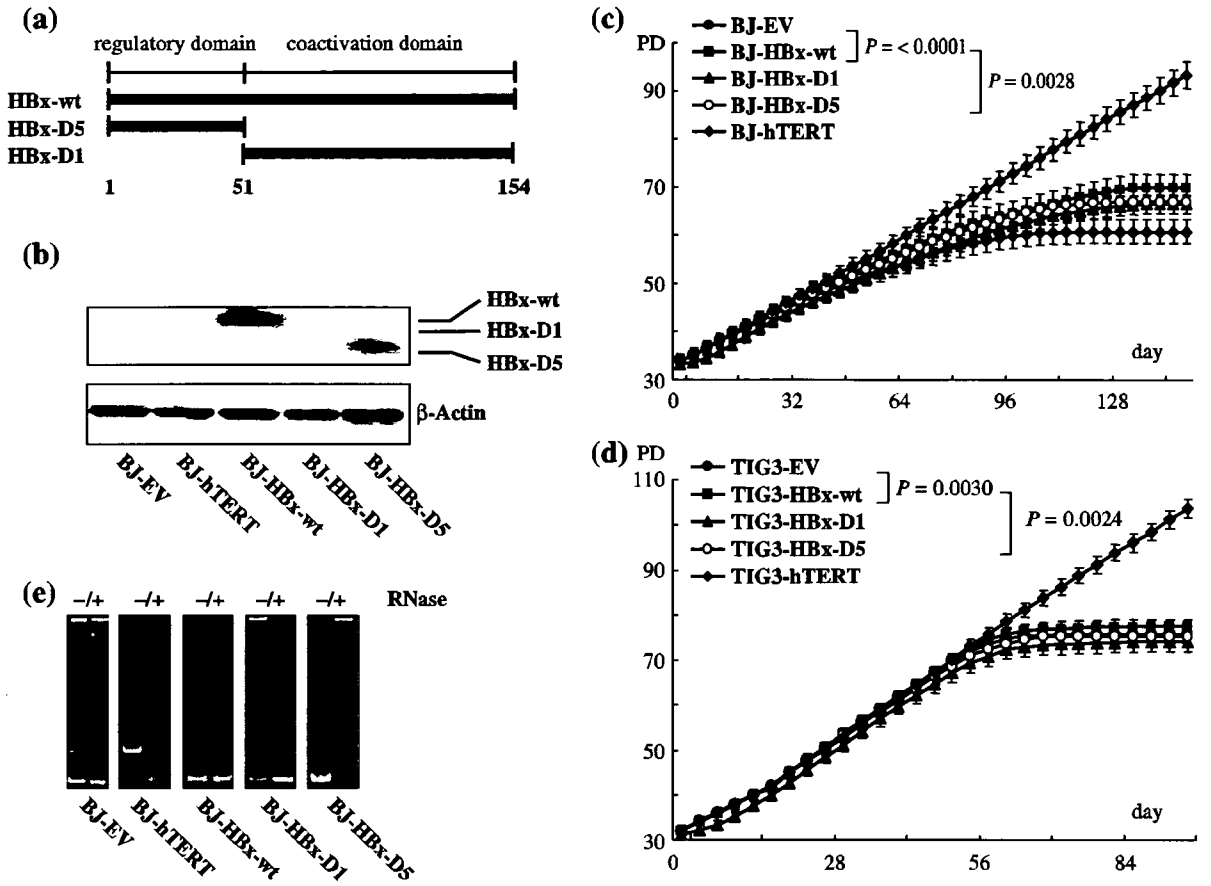

Fig. 1. Hepatitis B virus protein X (HBx) can not immortalize human primary cells, but weakly affects cellular senescence and telomerase activity. (a) Schematic representation of the HBx proteins.[5,8] The amino acids (aa) of full-length HBx (154 aa residues) and truncated HBx are shown. HBxD1 harbors the carboxy-terminal coactivation domain, spanning aa residues 51–154, whereas, HBxD5 harbors the amino-terminal negative regulatory domain, spanning aa residues 1–50. (b) Expression of HBx, HBx-D1 and HBx-D5 proteins in infected BJ cells. Total cell lysates of BJ cells infected with the empty vector (EV), human telomerase reverse transcriptase (hTERT), HBx, HBx-D1 and HBx-D5 expression retroviruses were fractionated by sodium dodecylsulfate–polyacrylamide gel electrophoresis and subjected to western blot analysis with anti-FLAG M2 antibody. (c) Effect of HBx on replicative senescence in BJ cells. BJ cells were infected with a control vector (filled circles) or hTERT (filled diamonds) and with a retrovirus encoding wild-type HBx (filled squares), HBx-D1 (filled triangles) or HBx-D5 (open circles). Cells infected with pBabe-puro- and pBabe-blast were selected with 1 μg/mL puromycin and 4 μg/mL blasticidin S, respectively. After 8 days of drug selection, triplicate samples of 1×10^5 cells were plated and grown under normal conditions (day 0). (d) Effect of HBx mutants on replicative senescence in TIG3 cells. Symbols are the same as in (c). (e) Telomerase activity in BJ cells as demonstrated by telomerase activity assay (TRAP). Total cell lysates (200 ng) prepared from BJ cells infected with control vector, hTERT, HBx, HBx-D1, and HBx-D5 were subjected to TRAP assay using a TRAPEZE kit (Intergen).

using human immortal cells. For this purpose, we used BJ-hTERT cells – these were BJ-derived cells immortalized by the introduction of hTERT, as characterized previously.[19] HBx-wt as well as its truncated mutants had no effect on cell proliferation, telomerase activity or cell transformation. Using the newly established TIG3-hTERT cells, we confirmed that the stable expression of HBx, XD1 or XD5 did not affect cell proliferation or cell transformation (data not shown). These results indicate the inability of HBx alone to transform these human immortalized cells.

Ability of HBx to overcome H-RAS^{V12}-induced senescence in BJ cells immortalized by hTERT Seeing as HBx did not exhibit the ability to immortalize primary human fibroblasts or to elicit transformation into hTERT-induced immortal primary human fibroblasts, we considered whether HBx functioned together with an oncogene and induced cell transformation. Senescence induced by active oncogene expression (OIS), such as oncogenic RAS, is one of the anticancer processes in which tumor suppressors and their related networks are involved, as demonstrated *in vitro* and recently also *in vivo*.[31,32] Overcoming OIS is critical for cellular transformation *in vitro* and cancerous cell proliferation *in vivo*.[31] Therefore, we addressed whether HBx has a collaborating role in transforming cells in the presence of oncogenic RAS or in overcoming RAS-induced senescence.

To examine the effect of HBx on RAS-induced senescence-like growth arrest, we introduced H-RAS^{V12} into BJ-hTERT, BJ-hTERT-HBx-wt, BJ-hTERT-HBx-D1 and BJ-hTERT-HBx-D5 cells using a retrovirus (Fig. 2d). BJ-hTERT cells expressing H-RAS^{V12} stopped proliferating within several days of RAS introduction. In contrast, BJ-hTERT cells expressing both H-RAS^{V12} and HBx-wt (BJ-hTERT + H-RAS^{V12} + HBx-wt) continued to proliferate to more than 80 PD (Fig. 2a). Although HBx-D1 also demonstrated the ability to overcome active RAS-induced senescence, HBx-D5 failed to overcome OIS (Fig. 2a). We also found that the growth rate of BJ-hTERT + H-RAS^{V12} + HBx-wt cells was much higher than that of BJ-hTERT + H-RAS^{V12} + HBx-D1 cells, probably reflecting the fact that some portion of the latter cells were positive for SA-β-gal (Fig. 2b,c). Consistent with this result, cells staining positive for SA-β-gal were significantly fewer in BJ-hTERT +

doi: 10.1111/j.1349-7006.2007.00579.x

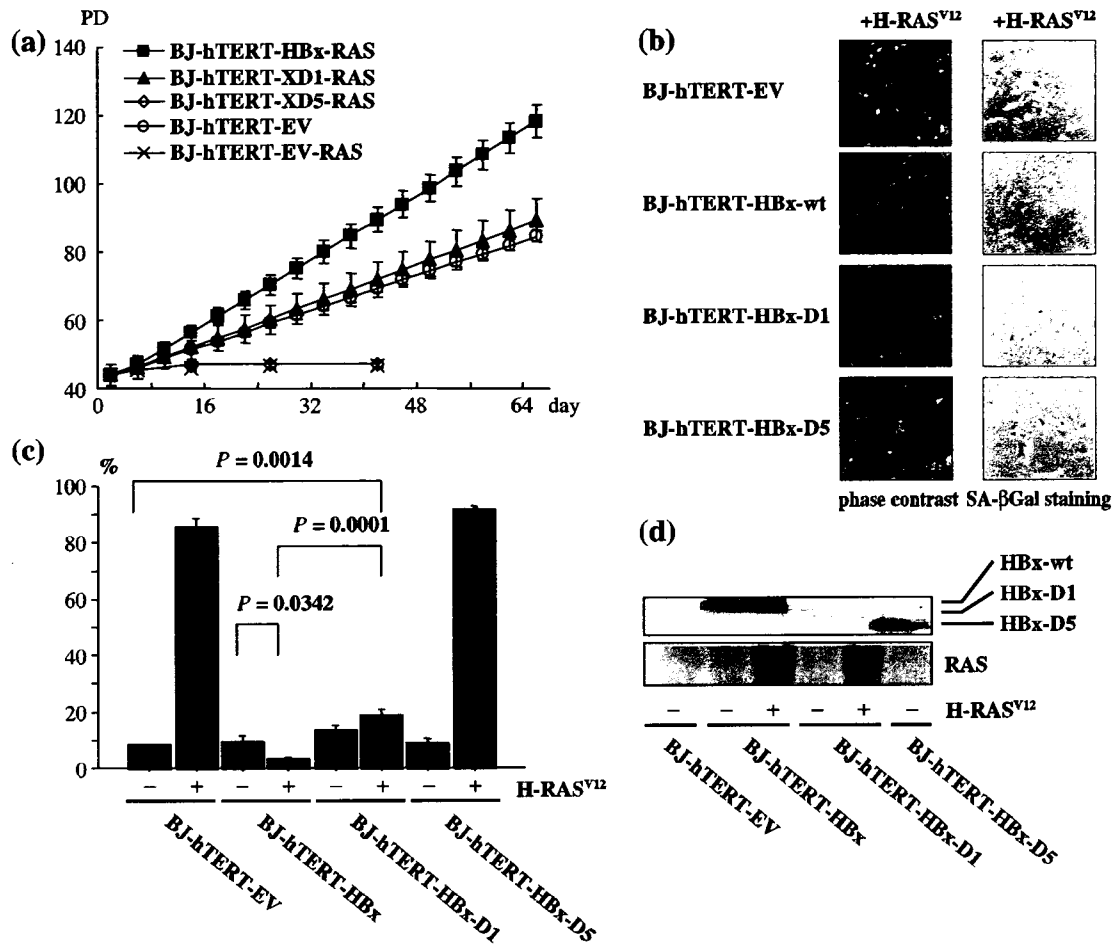

Fig. 2. Hepatitis B virus protein X (HBx) can overcome H-RAS^{V12}-induced cellular senescence of human immortalized cells. (a) Effect of HBx on H-RAS^{V12} induced senescence. BJ-human telomerase reverse transcriptase (hTERT) cells (open circles) and H-RAS^{V12}-induced BJ-hTERT-HBx-wt (filled squares), BJ-hTERT-HBx-D1 (filled triangles), BJ-hTERT-HBx-D5 (filled diamonds) cells and BJ-hTERT-empty vector (EV) (cross) are shown. After 10 days of drug selection at population doubling (PD) 42, triplicate samples of 1×10^5 cells were plated and grown under normal conditions (day 0). (b) HBx overcomes H-RAS^{V12}-induced senescence of human immortalized cells. H-RAS^{V12} and EV, full-length or truncated forms of HBx were introduced into BJ-hTERT cells. Left panel shows photographs 10 days after infection of the H-RAS^{V12}-expression retrovirus. Right panels show senescence-associated β-galactosidase (SA-β-Gal) staining 10 days after infection. (c) The percentage of cells positive for SA-β-Gal was determined in BJ cells stably expressing HBx-wt, HBx-D1, HBx-D5 or empty vector, with or without H-RAS^{V12} on day 9 after infection. Bars = mean ± SD. (d) Western blot analysis of RAS-induced cells. Total cell lysates from BJ-hTERT cells stably expressing HBx-wt, HBx-D1, HBx-D5 or EV together with or without H-RAS^{V12} were prepared and fractionated by sodium dodecylsulfate–polyacrylamide gel electrophoresis, then subjected to western blot analysis. HBx-wt, HBx-D1 and HBx-D5 were detected with anti-FLAG M2 antibody. RAS protein was detected with anti-RAS antibody.

H-RAS^{V12} + HBx-wt than in BJ-hTERT + H-RAS^{V12} + HBx-D1 (Fig. 2c). These results indicate that HBx-wt has the ability to overcome RAS-induced senescence. HBx-D1, the coactivator domain of HBx, seems to be indispensable and sufficient for overcoming RAS-induced senescence analyzed by the PD analysis, although HBx-D1 did not show the same ability as HBx-wt. The incomplete ability of HBx-D1 may be due to the low expression of HBx-D1 in the blastcidin S-selected clones in BJ-hTERT cells, as observed with the BJ cells (see Discussion).

HBx protein is required for anchorage-independent growth and tumor formation in nude mouse in response to H-RAS^{V12}. HBx can overcome RAS-induced senescence (examined by the PD analysis) and can indicate that HBx and RAS can induce cell transformation. Therefore, we examined whether BJ-hTERT + H-RAS^{V12} + HBx-wt and BJ-hTERT + H-RAS^{V12} + HBx-D1 cells can form colonies in soft agar. We found that BJ-hTERT + H-RAS^{V12} + HBx-wt cells showed cell number-dependent formation of colonies, which were much smaller size than those of control cells, BJ-hTERT + H-RAS^{V12} + SV40 LT + ST[20,33] (Fig. 3a,b). In contrast, BJ-hTERT + H-RAS^{V12} + HBx-D1 cells could not form colonies in soft agar (Fig. 3a), although these cells overcame RAS-induced senescence. This result strongly suggests that HBx-D1 is not equivalent to HBx-wt in its ability to make colonies in soft agar.

Next we tested the tumor-forming ability of BJ-hTERT + H-RAS^{V12} + HBx-wt or HBx-D1 cells in nude mice. BJ-hTERT + H-RAS^{V12} + HBx-wt cells were found to form tumors in four of eight mice, although these tumors grew much more slowly and were much smaller than those formed by BJ-hTERT + H-RAS^{V12} + SV40 LT + ST cells (eight of eight animals) (Fig. 3c). In contrast, BJ-hTERT + H-RAS^{V12} + HBx-D1 cells did not generate tumors in nude mice (Fig. 3c), consistent with the results of the soft-agar assay. These results indicate that HBx contributes to cellular transformation by collaborating with active RAS in human immortalized cells. To our knowledge, this is the first report showing that HBx plays a critical role in

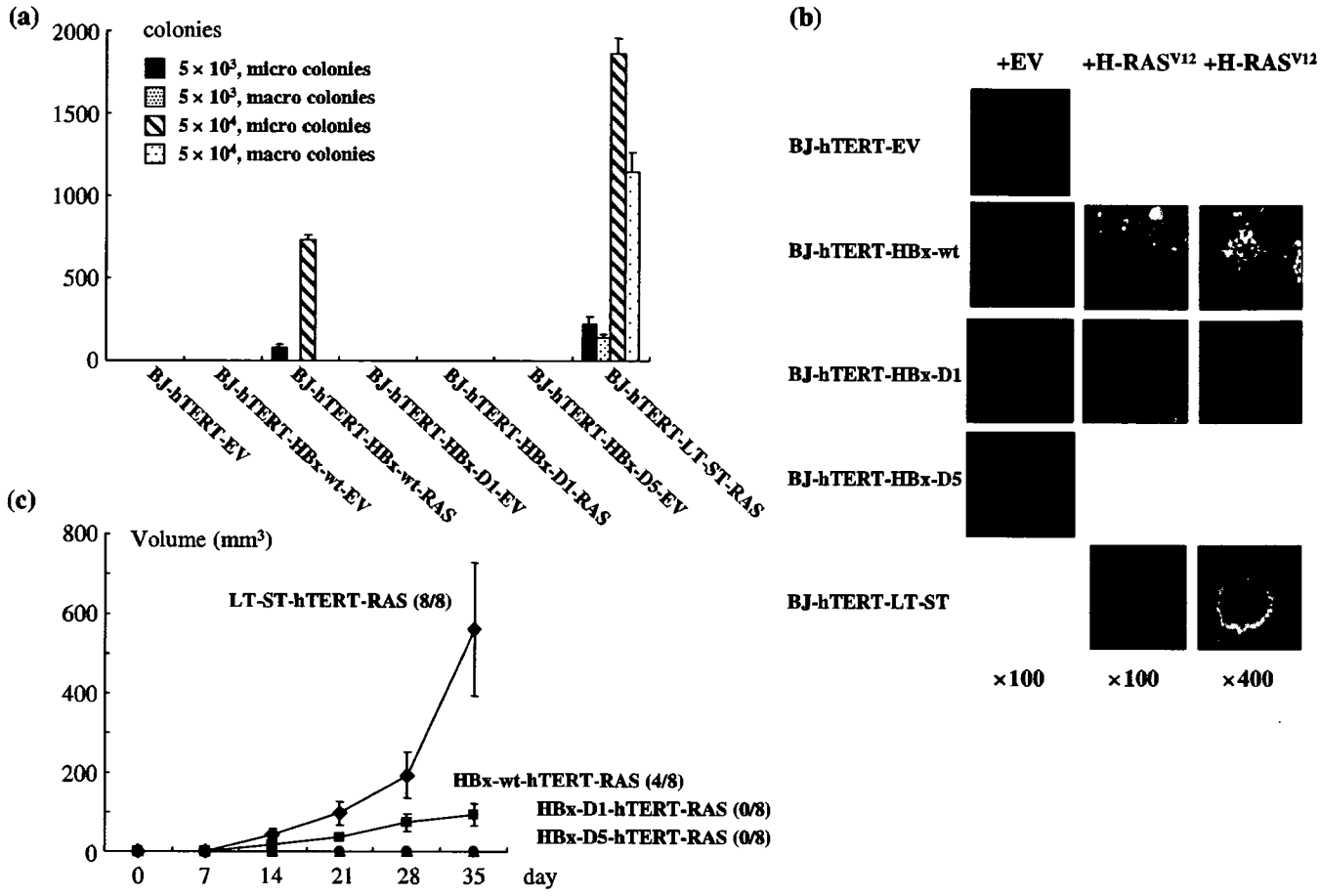

Fig. 3 (a,b) Anchorage-independent growth in soft agar and (c) tumorigenicity and tumor-forming ability in nude mice of cells expressing hepatitis B virus X protein (HBx) and H-RAS^{V12}. (a) Soft-agar assays were carried out as described in Materials and Methods.[19] After 3 weeks, colonies were counted and pictures were taken. The colony-forming ability of BJ-human telomerase reverse transcriptase (hTERT) cells stably expressing wild-type or truncated HBx with or without H-RAS^{V12} is indicated at the bottom. H-RAS^{V12}-introduced BJ-hTERT-LT-ST cells were the positive control. (b) Morphology of colonies in the soft-agar assay. Colonies were photographed 21 days after seeding. (c) Tumor formation in nude mice was carried out as described previously in Materials and Methods.[19,21] Tumor sizes were measured once a week. Each point on the graph represents the average volume of tumors. BJ-hTERT-LT-ST-RAS (filled diamonds), BJ-hTERT-HBx-RAS (filled squares), BJ-hTERT-HBx-D1 (filled circles), and BJ-hTERT (filled triangles) cells are shown. Error bars indicate the mean ± SD for each time point.

cellular transformation, collaborating with active RAS in human immortalized cells.

Effects of HBx on p16 and p21 expression and the ability of HBx to overcome RAS-induced senescence. Overexpression of RAS causes oncogene-induced premature senescence in normal human fibroblasts (Fig. 4c) and hTERT-immortalized human fibroblasts (Fig. 2a), but RAS failed to induce premature senescence in HBx-wt- or HBx-D1-introduced BJ-hTERT cells (Fig. 2a). We next examined the effect of stable expression of HBx in BJ cells with or without expression of hTERT, as interference with both the p53 and pRb pathways is necessary to avoid RAS-induced cellular senescence, in which p16 and p21 are the critical downstream effectors of pRb and p53, respectively. Expression of p16 and p21 was upregulated in HBx-wt- or HBx-D1-introduced BJ-hTERT cells; however, HBx-D5 has no ability to induce the expression of these genes. The presence of H-RAS^{V12} resulted in downregulation of the augmented expression of p16 and p21 in HBx-wt- or HBx-D1-introduced BJ cells and BJ-hTERT cells (Fig. 4a,b). These results suggest that HBx can suppress expression of p53, p16 and p21 in H-RAS^{V12}-introduced cells, contributing to overcoming RAS-induced senescence. Next we examined whether HBx-wt and H-RAS^{V12} not immortalized by hTERT were sufficient for cellular transformation. We introduced H-RAS^{V12} into BJ-HBx-wt, BJ-HBx-D1 and BJ-HBx-D5 cells and analyzed them by PD analysis and soft-agar colony assay. In the PD analysis, H-RAS^{V12}-introduced BJ-HBx-wt and BJ-HBx-D1 cells did overcome RAS-induced cellular senescence but stopped cell division at PD 62, which is approximately the cellular senescence of BJ cells (Figs 1c,4c), whereas H-RAS^{V12}-introduced BJ-HBx-D5 did not overcome senescence and stopped cell division. These results suggest that HBx can overcome RAS-induced senescence but can not immortalize the cells (Fig. 4c). In the soft-agar colony formation assay, BJ-HBx-wt-H-RAS^{V12} and BJ-HBx-D1-H-RAS^{V12} could but BJ-HBx-D5-H-RAS^{V12} could not form very tiny colonies, suggesting that HBx-wt and H-RAS^{V12} in the absence of hTERT may enable the cells to proliferate in an anchorage-independent manner (data not shown).

As HBx-D1, which was very weakly expressed, exhibited almost the same ability as HBx-wt to upregulate the tumor suppressor genes and to overcome RAS-induced senescence in these cells, we wondered whether HBx-D1 missing the N-terminal domain may have some negative effect on cell proliferation. Because the transient expression level of HBx-D1 in BJ cells was similar to those in HepG2 cells, as reported previously

doi: 10.1111/j.1349-7006.2007.00579.x

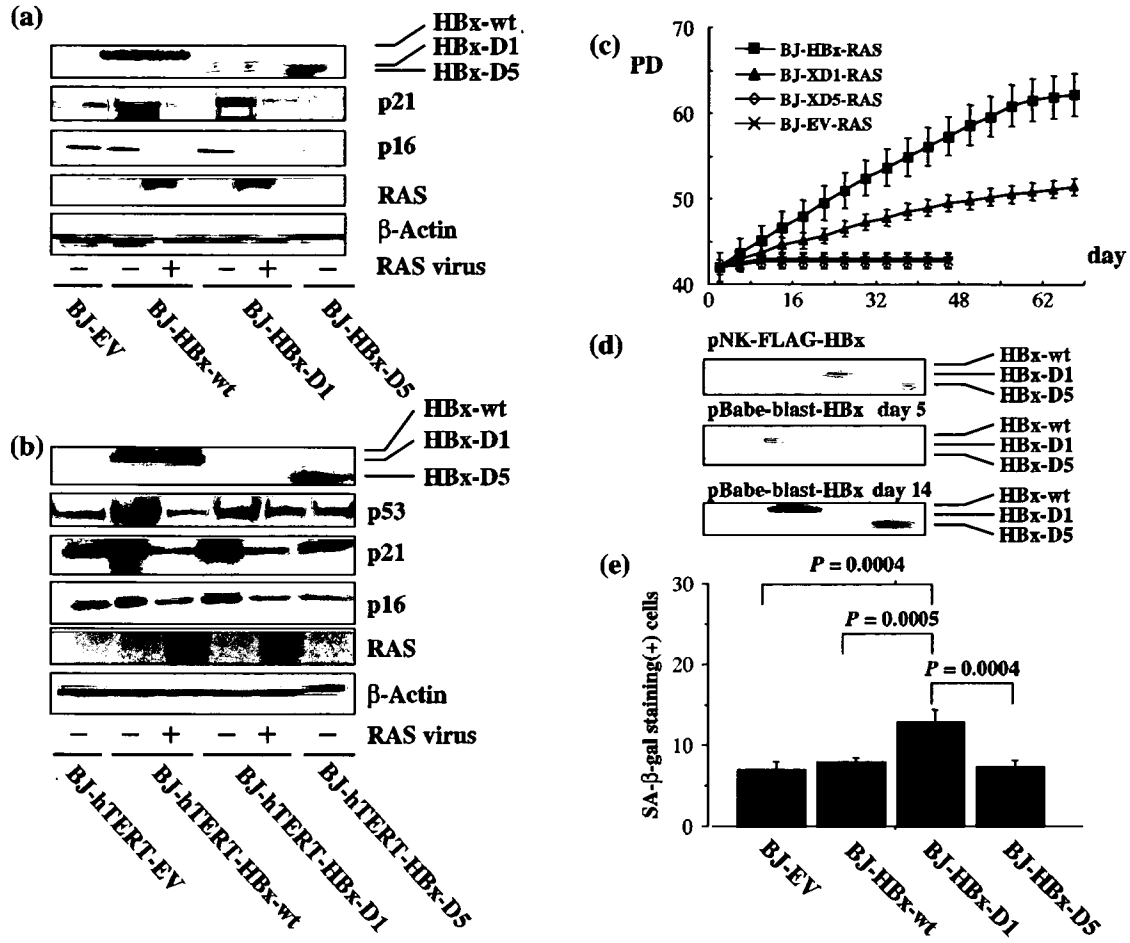

Fig. 4. Effect of hepatitis B virus X protein (HBx) on p16 and p21 expression and the ability of HBx to overcome H-RAS^{V12}-induced cellular senescence of human normal cells. Total cell lysates from BJ-human telomerase reverse transcriptase (hTERT) cells stably expressing HBx-wt, HBx-D1, HBx-D5 or empty vector together with or without H-RAS^{V12} were prepared, and fractionated by sodium dodecylsulfate–polyacrylamide gel electrophoresis (SDS-PAGE), then subjected to western blot analysis. Expression of (a) p16 and p21 proteins and (b) p53, p16 and p21 proteins. (c) Effect of HBx on H-RAS^{V12}-induced senescence. Population doublings (PD) of H-RAS^{V12}-induced BJ-HBx-wt (filled squares), BJ-HBx-D1 (filled triangles), BJ-HBx-D5 (open diamonds) and BJ-EV (cross) cells are shown. After 10 days of drug selection, at PD 44, triplicate samples of 1×10^5 cells were plated and grown under normal conditions (day 0). (d) Expression of HBx, HBx-D1 and HBx-D5 proteins in infected BJ cells. Total cell lysates of BJ cells transfected with mammalian expression plasmids of FLAG-HBx-wt, FLAG-HBx-D1 and FLAG-HBx-D5 were fractionated by SDS-PAGE and subjected to western blot analysis with anti-FLAG M2 antibody (upper panel). Total cell lysates of BJ cells infected with the empty vector (EV), HBx-wt, HBx-D1 and HBx-D5 expression retroviruses were fractionated by SDS-PAGE and subjected to western blot analysis with anti-FLAG M2 antibody (middle and bottom panel). (e) The percentage of cells positive for senescence-associated β-galactosidase (SA-β-Gal) was determined in BJ cells stably expressing HBx-wt, HBx-D1, HBx-D5 or empty vector (EV) on day 40 after infection. Bars = mean ± SD.

(Fig. 4d),[8] it was not due to the construct design of the vector. The expression of HBx-D1 was slightly lower than those of HBx-wt and HBx-D5 on day 5 after selection, much lower on day 10 after selection (data not shown). On day 14 after selection, the expression of HBx-D1 reached the lowest level, and after day 14 that expression level was kept (Figs 1b,4d). HBx-D1-introduced BJ cells grew slower than HBx-wt- or HBx-D5-introduced BJ cells (data not shown) and contained more SA-β-Gal-positive cells during proliferation (Fig. 4e). These results suggest that cells expressing lower levels of HBx-D1 proliferated more than cells expressing higher levels of HBx-D1, due to some toxic or antiproliferative effect of the coactivation domain of HBx in the human primary cells (see Discussion).

Important region of HBx for overcoming cellular senescence and anchorage-independent growth. As HBx exhibited the ability to overcome active RAS-induced senescence, we next tried to identify the critical regions of HBx for overcoming cellular senescence. BJ-hTERT cells were infected with retroviruses expressing one of the clustered alanine-substituted mutants covering all parts of HBx,[34] and a series of cell clones stably expressing these HBx-cm mutants, BJ-hTERT-HBx-cm, was established (Fig. 5). H-RAS^{V12} was then introduced into BJ-hTERT-HBx-cm1 to BJ-hTERT-HBx-cm21 cells and cell proliferation was examined. The regions covering HBx-cm8 to HBx-cm10, and those covering HBx-cm19 to HBx-cm21 were found to be not critical for overcoming active RAS-induced senescence and anchorage-independent growth as the BJ-hTERT-RAS clones expressing these HBx-cm mutants proliferated and formed colonies in soft agar, similar to BJ-hTERT-HBx-wt-H-RAS^{V12} cells. The BJ-hTERT-RAS clones expressing HBx-cm1 to HBx-cm7, and those expressing HBx-cm14 to HBx-cm16, were like BJ-hTERT-HBx-D1-RAS, which can grow but at a much reduced rate compared with BJ-hTERT-HBx-RAS cells. The HBx regions covering HBx-cm11 to HBx-cm13, HBx-cm17

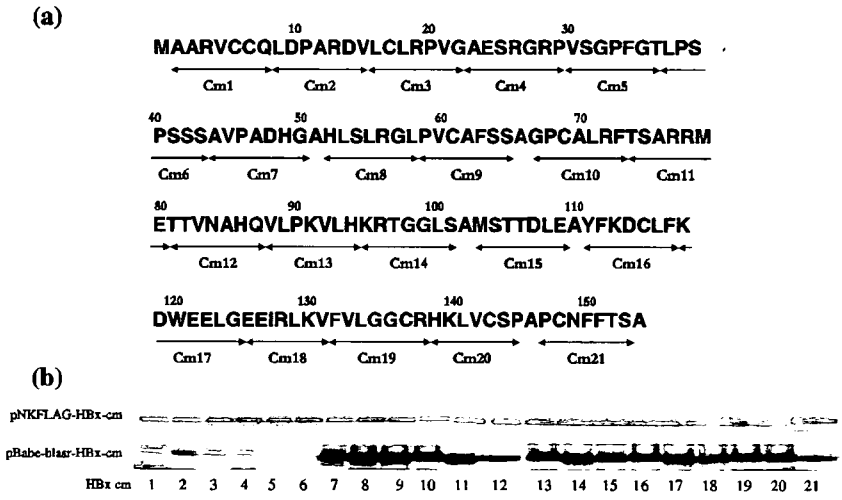

Fig. 5. Expression of hepatitis B virus X protein (HBx) library of clustered alanine substitution mutants in BJ-human telomerase reverse transcriptase (hTERT) cells. (a) Schematic representations of a series of clustered alanine substitution mutants (cm1 to cm21) of HBx. The amino acid locations of the clustered mutations are shown. (b) Detection of the mutated HBx proteins. Total cell lysates prepared from BJ-hTERT cells transfected with the mutant HBx expression vectors were fractionated by sodium dodecylsulfate–polyacrylamide gel electrophoresis and subjected to western blot analysis with anti-FLAG M2 antibody.

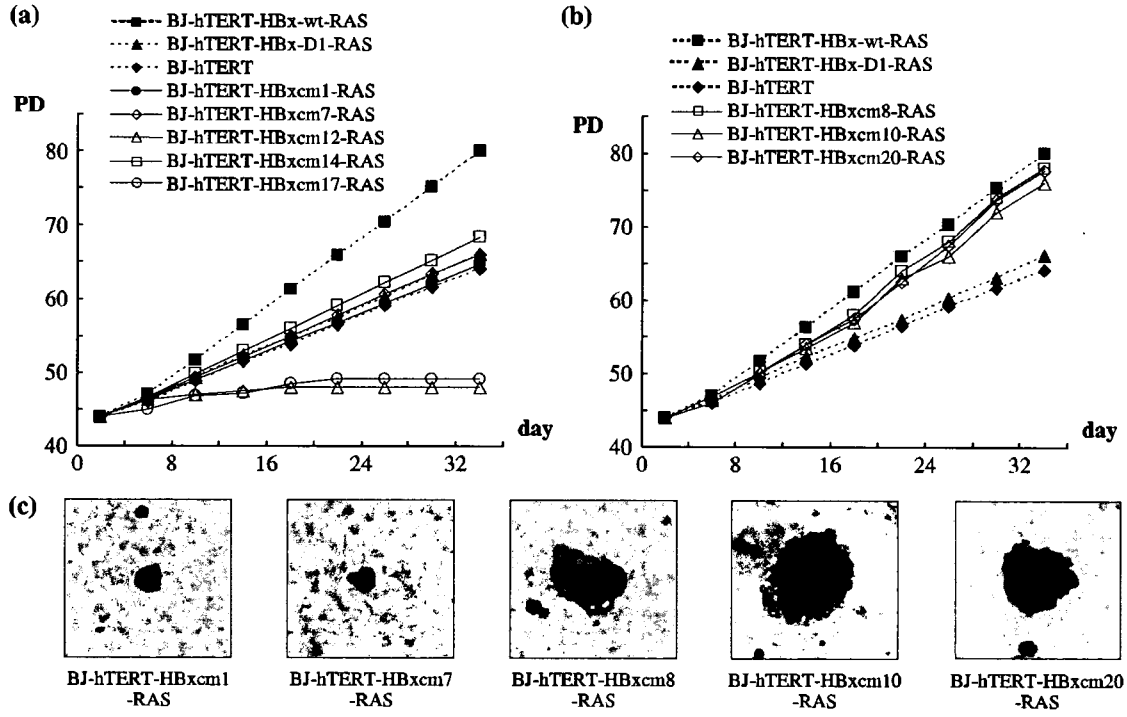

Fig. 6. Critical regions of hepatitis B virus X protein (HBx)-wt for tumorigenic function. (a) Effect of HBx-cm1–7 and HBx-cm11–18 failed to overcome H-RAS^{V12}-induced cellular senescence. Cell proliferation curves of several HBx-cm clones introduced with BJ-human telomerase reverse transcriptase (hTERT)-H-RAS$^{V(12)}$ in addition to those of BJ-hTERT cells (filled diamonds), H-RAS^{V12}-introduced BJ-hTERT-HBx-wt cells (filled squares) and BJ-hTERT-HBx-D1 cells (filled triangles) are shown. HBx-cm1, -cm7, -cm12, -cm14 and -cm17 were selected. HBx-cm1 (closed circles) and HBx-cm7 (open diamonds) represent HBx-cm1–7-introduced BJ-hTERT-H-RAS^{V12} cells. HBx-cm12 (open triangles) represents HBx-cm11–13-introduced BJ-hTERT-H-RAS^{V12} cells. HBx-cm14 (open squares) represents HBx-cm14–16-introduced BJ-hTERT-H-RAS^{V12} cells. HBx-cm17 (open circles) represents HBx-cm17 and HBx-cm18-introduced BJ-hTERT-H-RAS^{V12} cells. pBabe-puro-RAS-infected cells were selected with 1 μg/mL puromycin. After 10 days of drug selection at population doubling (PD) 44, triplicate samples of 1×10^5 cells were plated and grown under normal conditions. (b) Effect of HBx-cm8–10 and HBx-cm19–21 overcomes H-RAS^{V12}-induced cellular senescence. Cell proliferation curves of several HBx-cm clones introduced into BJ-hTERT-H-RAS^{V12} in addition to those of BJ-hTERT cells (filled diamonds), H-RAS^{V12}-introduced BJ-hTERT-HBx-wt cells (filled square) and BJ-hTERT-HBx-D1 cells (filled triangles) are shown. HBx-cm8 (open squares) and HBx-cm10 (open triangles) represent HBx-cm8–10-introduced BJ-hTERT-H-RAS^{V12} cells. HBx-cm20 (open diamonds) represents HBx-cm19–21-introduced BJ-hTERT-H-RAS^{V12} cells.

and HBx-cm18 were found to be critical for overcoming active RAS-induced senescence as the BJ-hTERT-RAS clones expressing these HBx-cm mutants failed to proliferate, meaning that these had no ability to overcome active RAS-induced cellular senescence at all (Fig. 6) (Table 1). Among the BJ-hTERT-HBx-cm cells, expression levels of HBx-cm1 to HBx-cm6 were very weak, like that of HBx-D1. Furthermore, the protein bands of HBx-cm1 to HBx-cm5 migrated slightly slower than those of HBx-cm6 and the other HBx-cm mutants in the coactivation domain in SDS-PAGE analysis (see Discussion).

doi: 10.1111/j.1349-7006.2007.00579.x

Table 1. Degree of proliferation of H-RAS^{V12}-introduced BJ-hTERT-HBx-cm cells

Cell type	Degree of proliferation
HBx-cm1[†]	+[‡]
HBx-cm2	+
HBx-cm3	+
HBx-cm4	+
HBx-cm5	+
HBx-cm6	+
HBx-cm7	+
HBx-cm8	++[§]
HBx-cm9	++
HBx-cm10	++
HBx-cm11	–
HBx-cm12	–[¶]
HBx-cm13	–
HBx-cm14	+
HBx-cm15	+
HBx-cm16	+
HBx-cm17	–
HBx-cm18	–
HBx-cm19	++
HBx-cm20	++
HBx-cm21	++

[†]HBx-cm1–21 in this table represent HBx-cm1–21-introduced BJ-hTERT-H-RAS^{V12} cells. [‡]Same as BJ-hTERT-HBx-D1-H-RAS^{V12} cells. [§]Same as BJ-hTERT-HBx-wt-H-RAS^{V12} cells. [¶]Senescence.

Discussion

Hepatitis B virus X protein has long been suspected to be positively involved in HBV-associated HCC, but its molecular role in hepatocarcinogenesis remains unclear. Although HBx is involved directly in the transformation of immortal rodent cells *in vitro* and in tumor formation in the livers of nude mice, the oncogenic activity of HBx itself remains to be elicited as the reproducibility of these experiments has been seriously controversial.[5] Furthermore, the positive role of HBx has not been addressed with human primary cells or human immortal cells. To our knowledge, our report is the first to show that HBx retains the ability to overcome RAS-induced senescence of immortalized human cells, although it is not sufficient for immortalizing human primary cells or transforming human immortal cells. hTERT-immortalized human cells stably expressing HBx-wt and RAS can form colonies in soft agar and tumors in nude mice in a cell-number-dependent manner. HBx can overcome RAS-induced senescence of BJ cells, but HBx-wt and active RAS could not immortalize the human fibroblasts. Although our findings are different to a report showing that HBx itself retains the transforming ability in NIH3T3 cells,[9] they are similar to results in rodent immortal embryonic fibroblast cells.[10]

To determine the region of HBx responsible for the ability to overcome RAS-induced senescence, we used two truncation mutants: HBx-D1 (aa 51–154), which exhibits transcriptional coactivation function and augments HBV transcription and replication,[8] and HBx-D5 (aa 1–50), which harbors the negative regulatory domain of transcriptional modulation.[6] When HBx-D1 and H-RAS^{V12} were introduced into BJ-hTERT cells, HBx-D1 was similar to wild-type HBx in overcoming RAS-induced senescence in the PD analysis and in SA-β-gal staining. Therefore, HBx-D1 alone seems to be sufficient for overcoming active RAS-induced senescence and for anchorage-independent growth, but it is not sufficient for BJ-hTERT + H-RAS^{V12} + HBx-D1 cells to form visible colonies in soft agar and tumors in nude mice. HBx alone may be sufficient for overcoming RAS-induced senescence, but hTERT is required for immortal proliferation of the transformed cells with H-RAS^{V12} and HBx. As HBx-D1 exhibits a similar ability to HBx-wt in overcoming RAS-induced senescence and anchorage-independent growth, but not in immortalizing human fibroblasts, HBx-D1 may harbor all of the critical abilities of HBx. However, HBx-D1 is different from HBx-wt in the ability to form visible colonies in soft agar and to form tumors in nude mice.

The coactivation function was recently mapped by scanning a HBx library of clustered alanine substitution mutants (HBx-cm library), and two separate sequences in HBx-D1 were found to be critical.[8] Using the same HBx-cm library, we attempted to map the sequences critical for overcoming RAS-induced senescence. We have identified three different phenotypes among the HBx-cm mutants: those phenotypes are like HBx-wt, HBx-D1 and HBx-D5 (Fig. 6). HBx-cm mutations within the D5 region, cm1 to cm7, have the ability to partially overcome OIS, whereas those within the D1 region (cm8–10, cm14–16 and cm 19–21) fail to exhibit the overcoming ability. The HBx-D5 phenotype is even found among the HBx-cm mutants (cm13, cm17 and cm18) that are defective in the coactivation function.[8] These results indicate that the ability to fully overcome OIS requires two putative functions carried by the D1 and D5 regions of the HBx protein. Because HBx-D5 does not have a positive or negative effect on RAS-induced senescence (Figs 2,3,4c), the negative regulatory domain may be active only in full-length HBx. The very low expression of HBx-D1 in human primary cells and hTERT-immortalized cells may be due to the selection result of clones, reflecting that a high level of HBx-D1 protein was eliminated due to a toxic effect of the coactivation domain,[5] or due to deletion of the N-terminal domain that has some critical role in stabilizing HBx in the expression system. Both of these may actually occur. The former is supported by the enrichment of cells expressing HBx-D1 during the early stages of drug selection. The latter is highly possible as expression levels of HBx-cm1 to HBx-cm6 covering most of the N-terminal domain were very low, as for HBx-D1. Pang *et al.* recently reported a stabilization mechanism of HBx through direct interaction with Pin1,[35] which binds phosphorylated serine and the next proline. The target serine residue is within the N-terminal domain or within the region covered by HBx-cm6. Interestingly, the HBx-cm1 to HBx-cm5 bands migrated more slowly than the HBx-cm6 band (Fig. 5b), supporting the possibility that the N-terminal domain may be critical for Pin1 binding to stabilize HBx. One interesting possibility that remains to be tested is that activation of the degradation pathway of HBx causes the toxic effect on cell proliferation. This possibility may explain the low expression of HBx-D1 and the cm mutants in the N-terminal domain. In this context, it remains unclear at present the reason for the rather stable expression of two bands of HBx-cm7 that seem to confer the same phenotype as HBx-D1 in the characterization of the cells.

The region of D1 that is responsible for overcoming RAS-induced senescence should be defined. Because some HBx-cm mutants defective in coactivation function still exhibit the ability to overcome OIS, it seems that the coactivation function is dispensable for the role. More than a dozen host factors have been reported to interact directly with the HBx-D1 region, including p53,[36,37] Smad4,[38] DDB1,[39,40] and two core subunits of the proteasome.[5] It is especially important to determine whether the binding of HBx to p53 is responsible for the ability to overcome RAS-induced senescence, as the direct binding of p53 to HBx was found to suppress p53-dependent gene activation.[5,37]

Although we have shown here that the D5 region of HBx has an indispensable biological role in anchorage-independent cell growth, the critical role of the D5 region in overcoming OIS remains obscure. The ability of the D5 region in full-length HBx

to support anchorage-independent growth will provide a good experimental system for revealing the function of the negative regulatory domain of HBx, as no host factor has been reported to interact specifically with the D5 region.

Our results clearly indicate that HBx retains the ability to overcome RAS-induced senescence in human cells immortalized by hTERT, although HBx alone could neither immortalize nor transform human cells. The ability of HBx to collaborate with active RAS in cell transformation may explain its role in hepatocellular carcinogenesis. Our findings, however, were obtained using an experimental model with immortalized cells derived from human fibroblasts. Our results may not reflect the role of HBx in HBV-infected liver, as overcoming the processes of OIS seems to vary with tissue and tumor type.[41] The role of HBx should therefore be addressed using human hepatocytes and immortalized human hepatocytes. The former, however, are quite difficult to obtain whereas the latter are available at present. It had been immortalized by introducing the other viral oncogene SV LT.[42,43]

Acknowledgments

We thank K. Masutomi and W. C. Hahn for kindly providing the retroviral vectors and human immortal cell lines, T. B. S. Yen (UCSF, USA) and H. Tang (Sichuan University, China) and the members of the Division for critical discussions, and Ms Yasukawa and Ms Kuwabara for excellent technical assistance. This work was supported in part by a Grant-in-aid for Scientific Research and Development (B) (1790031) and a Grant-in-aid for Scientific Research on Priority Areas (C) (12213050 and 17013035) from the Ministry of Education, Culture, Sports, and Technology.

References

1 Seeger C, Mason WS. Hepatitis B virus biology. *Microbiol Mol Biol Rev* 2000; **64**: 51–68.
2 Nassal M, Schaller H. Hepatitis B virus replication. *Trends Microbiol* 1993; **1**: 221–8.
3 Arbuthnot P, Kew M. Hepatitis B virus and hepatocellular carcinoma. *Int J Exp Pathol* 2001; **82**: 77–100.
4 Murakami S. Hepatitis B virus X protein: structure, function and biology. *Intervirology* 1999; **42**: 81–99.
5 Murakami S. Hepatitis B virus X protein: a multifunctional viral regulator. *J Gastroenterol* 2001; **36**: 651–60.
6 Murakami S, Cheong JH, Kaneko S. Human hepatitis virus X gene encodes a regulatory domain that represses transactivation of X protein. *J Biol Chem* 1994; **269**: 15 118–23.
7 Lin Y, Tang H, Nomura T *et al.* The hepatitis B virus X protein is a co-activator of activated transcription that modulates the transcription machinery and distal binding activators. *J Biol Chem* 1998; **273**: 27 097–103.
8 Tang H, Delgermaa L, Huang F *et al.* The transcriptional transactivation function of HBx protein is important for its augmentation role in hepatitis B virus replication. *J Virol* 2005; **79**: 5548–56.
9 Shirakata Y, Kawada M, Fujiki Y *et al.* The X gene of hepatitis B virus induced growth stimulation and tumorigenic transformation of mouse NIH3T3 cells. *Jpn J Cancer Res* 1989; **80**: 617–21.
10 Kim YC, Song KS, Yoon G *et al.* Activated ras oncogene collaborates with HBx gene of hepatitis B virus to transform cells by suppressing HBx-mediated apoptosis. *Oncogene* 2001; **20**: 16–23.
11 Kim CM, Koike K, Saito I, Miyamura T, Jay G. HBx gene of hepatitis B virus induces liver cancer in transgenic mice. *Nature* 1991; **351**: 317–20.
12 Yu DY, Moon HB, Son JK *et al.* Incidence of hepatocellular carcinoma in transgenic mice expressing the hepatitis B virus X-protein. *J Hepatol* 1999; **31**: 123–32.
13 Gottlob K, Pagano S, Levrero M, Graessmann A. Hepatitis B virus X protein transcription activation domains are neither required nor sufficient for cell transformation. *Cancer Res* 1998; **58**: 3566–70.
14 Slagle BL, Lee TH, Medina D, Finegold MJ, Butel JS. Increased sensitivity to the hepatocarcinogen diethylnitrosamine in transgenic mice carrying the hepatitis B virus X gene. *Mol Carcinog* 1996; **15**: 261–9.
15 Terradillos O, Billet O, Renard CA *et al.* The hepatitis B virus X gene potentiates c-myc-induced liver oncogenesis in transgenic mice. *Oncogene* 1997; **14**: 395–404.
16 Artandi SE, DePinho RA. Mice without telomerase: what can they teach us about human cancer? *Nat Med* 2000; **6**: 852–5.
17 Balmain A, Harris CC. Carcinogenesis in mouse and human cells: parallels and paradoxes. *Carcinogenesis* 2000; **21**: 371–7.
18 Rangarajan A, Hong SJ, Gifford A, Weinberg RA. Species- and cell type-specific requirements for cellular transformation. *Cancer Cell* 2004; **6**: 171–83.
19 Hahn WC, Counter CM, Lundberg AS, Beijersbergen RL, Brooks MW, Weinberg RA. Creation of human tumour cells with defined genetic elements. *Nature* 1999; **400**: 464–8.
20 Wei W, Jobling WA, Chen W, Hahn WC, Sedivy JM. Abolition of cyclin-dependent kinase inhibitor p16Ink4a and p21Cip1/Waf1 functions permits Ras-induced anchorage-independent growth in telomerase-immortalized human fibroblasts. *Mol Cell Biol* 2003; **23**: 2859–70.
21 Akagi T, Sasai K, Hanafusa H. Refractory nature of normal human diploid fibroblasts with respect to oncogene-mediated transformation. *Proc Natl Acad Sci USA* 2003; **100**: 13 567–72.
22 Greenberg RA, Allsopp RC, Chin L, Morin GB, DePinho RA. Expression of mouse telomerase reverse transcriptase during development, differentiation and proliferation. *Oncogene* 1998; **16**: 1723–30.
23 Newbold RF. Genetic control of telomerase and replicative senescence in human and rodent cells. *Ciba Found Symp* 1997; **211**: 177–89.
24 Harvey M, Sands AT, Weiss RS. *et al. In vitro* growth characteristics of embryo fibroblasts isolated from p53-deficient mice. *Oncogene* 1993; **8**: 2457–67.
25 Kamijo T, Zindy F, Roussel MF. *et al.* Tumor suppression at the mouse INK4a locus mediated by the alternative reading frame product p19ARF. *Cell* 1997; **91**: 649–59.
26 Sedivy JM. Can ends justify the means? Telomeres and the mechanisms of replicative senescence and immortalization in mammalian cells. *Proc Natl Acad Sci USA* 1998; **95**: 9078–81.
27 Shay JW, Wright WE, Werbin H. Defining the molecular mechanisms of human cell immortalization. *Biochim Biophys Acta* 1991; **1072**: 1–7.
28 Bodnar AG, Ouellette M, Frolkis M *et al.* Extension of life-span by introduction of telomerase into normal human cells. *Science* 1998; **279**: 349–52.
29 Halvorsen TL, Leibowitz G, Levine F. Telomerase activity is sufficient to allow transformed cells to escape from crisis. *Mol Cell Biol* 1999; **19**: 1864–70.
30 Hahn WC. Role of telomeres and telomerase in the pathogenesis of human cancer. *J Clin Oncol* 2003; **21**: 2034–43.
31 Sharpless NE, DePinho RA. Cancer: crime and punishment. *Nature* 2005; **436**: 636–7.
32 Braig M, Lee S, Loddenkemper C *et al.* Oncogene-induced senescence as an initial barrier in lymphoma development. *Nature* 2005; **436**: 660–5.
33 Hahn WC, Dessain SK, Brooks MW *et al.* Enumeration of the simian virus 40 early region elements necessary for human cell transformation. *Mol Cell Biol* 2002; **22**: 2111–23.
34 Tang H, Oishi N, Kaneko S, Murakami S. Molecular functions and biological roles of hepatitis B virus X protein. *Cancer Sci* 2006; **97**: 977–83.
35 Pang R, Lee TK, Poon RT *et al.* Pin1 interacts with a specific serine-proline motif of hepatitis B virus X-protein to enhance hepatocarcinogenesis. *Gastroenterology* 2007; **132**: 1088–1103.
36 Elmore LW, Hancock AR, Chang SF *et al.* Hepatitis B virus X protein and p53 tumor suppressor interactions in the modulation of apoptosis. *Proc Natl Acad Sci USA* 1997; **94**: 14 707–12.
37 Lin Y, Nomura T, Yamashita T, Dorjsuren D, Tang H, Murakami S. The transactivation and p53-interacting functions of hepatitis B virus X protein are mutually interfering but distinct. *Cancer Res* 1997; **57**: 5137–42.
38 Lee DK, Park SH, Yi Y *et al.* The hepatitis B virus encoded oncoprotein pX amplifies TGF-beta family signaling through direct interaction with Smad4: potential mechanism of hepatitis B virus-induced liver fibrosis. *Genes Dev* 2001; **15**: 455–66.
39 Lee TH, Elledge SJ, Butel JS. Hepatitis B virus X protein interacts with a probable cellular DNA repair protein. *J Virol* 1995; **69**: 1107–14.
40 Leupin O, Bontron S, Schaeffer C, Strubin M. Hepatitis B virus X protein stimulates viral genome replication via a DDB1-dependent pathway distinct from that leading to cell death. *J Virol* 2005; **79**: 4238–45.
41 DePinho RA. The age of cancer. *Nature* 2000; **408**: 248–54.
42 Kobayashi N, Noguchi H, Watanabe T *et al.* A new approach to develop a biohybrid artificial liver using a tightly regulated human hepatocyte cell line. *Hum Cell* 2000; **13**: 229–35.
43 Kobayashi N, Miyazaki M, Fukaya K *et al.* Treatment of surgically induced acute liver failure with transplantation of highly differentiated immortalized human hepatocytes. *Cell Transplant* 2000; **9**: 733–5.

doi: 10.1111/j.1349-7006.2007.00579.x

Available online at www.sciencedirect.com
ScienceDirect
ELSEVIER
Biochemical and Biophysical Research Communications 361 (2007) 379–384
BBRC
www.elsevier.com/locate/ybbrc

Gene expression profiles in peripheral blood mononuclear cells reflect the pathophysiology of type 2 diabetes

Toshinari Takamura [a,*], Masao Honda [a], Yoshio Sakai [a], Hitoshi Ando [a], Akiko Shimizu [a], Tsuguhito Ota [a], Masaru Sakurai [a], Hirofumi Misu [a], Seiichiro Kurita [a], Naoto Matsuzawa-Nagata [a], Masahiro Uchikata [a], Seiji Nakamura [a,b], Ryo Matoba [b], Motohiko Tanino [b], Ken-ichi Matsubara [b], Shuichi Kaneko [a]

[a] *Department of Disease Control and Homeostasis, Kanazawa University Graduate School of Medical Science, 13-1 Takara-machi, Kanazawa, Ishikawa 920 8641, Japan*
[b] *DNA Chip Research Inc., Yokohama, Japan*

Received 19 June 2007
Available online 16 July 2007

Abstract

We hypothesized that systemically circulating peripheral blood mononuclear cells (PBMCs) reflect the pathophysiology of type 2 diabetes. PBMCs were obtained from 18 patients with type 2 diabetes and 16 non-diabetic subjects. The expression of genes in the PBMCs was analyzed by using a DNA chip followed by statistical analysis for specific gene sets for biological categories. The only gene set coordinately up-regulated by the existence of diabetes and down-regulated by glycemic control consisted of 48 genes involved in the c-Jun N-terminal kinase (JNK) pathway. In contrast, the only gene set coordinately down-regulated by the existence of diabetes, but not altered by glycemic control consisted of 92 genes involved in the mitochondrial oxidative phosphorylation (OXPHOS) pathway. Our findings suggest that genes involved in the JNK and OXPHOS pathways of PBMCs may be surrogate transcriptional markers for hyperglycemia-induced oxidative stress and morbidity of type 2 diabetes, respectively.

Keywords: c-Jun N-terminal kinase; Diabetes; DNA chip; Gene expression; Glycemic control; Oxidative stress; Mitochondria; Oxidative phosphorylation; Peripheral blood mononuclear cell

Diabetes is caused by absolute and/or relative deficiency of insulin action due to genetic disposition and environmental factors. Therefore, the diagnosis of diabetes requires a comprehensive understanding of hereditary aspects as well as habit and environmental effects. A long-term duration of diabetes causes chronic vascular complications. The underlying mechanism causing diabetic pathophysiology involves hyperglycemia itself and protein glycation. Additionally, bioactive mediators such as plasminogen activator-1, vascular endothelial growth factor, fatty acids, and adipocytokines secreted from the liver and adipose tissue can cause oxidative stress and thereby promote insulin resistance [1] and vascular complications [2]. We revealed one of the systemic manifestations of diabetes in our previous work, which showed that the hepatic gene expression profile of patients with type 2 diabetes is altered from that of patients without diabetes [3,4]. The livers of patients with type 2 diabetes had gene expression profiles indicative of increased angiogenesis, a reduced stress-defence system [3], and altered mitochondrial oxidative phosphorylation (OXPHOS) [4].

Owing to the multiple and complicated causes of the onset of diabetes, the search for conventional biomarkers that reflect diabetic pathophysiology and predict prognosis is an important issue. Glycated proteins such as haemoglobin A_{1C} HbA_{1C} and glucoalbumin are used as surrogate markers for long-term glycemic control [5,6]. Albuminuria

* Corresponding author. Fax: +81 76 234 4250.
E-mail address: ttakamura@m-kanazawa.jp (T. Takamura).

0006-291X/$ - see front matter © 2007 Elsevier Inc. All rights reserved.
doi:10.1016/j.bbrc.2007.07.006

is predictive of not only future diabetic nephropathy but also cardiovascular events [7,8]. High-sensitivity C-reactive protein (hs-CRP) has been found to be an independent indicator of coronary heart disease [9]. However, the use and clinical significance of these markers are limited.

Systemically circulating peripheral blood mononuclear cells (PBMCs) are considered to be a unique tissue affected by the host condition and may reflect oxidative stress caused by high levels of glucose, insulin, free fatty acids, and tissue-derived circulating bioactive mediators. To verify the hypothesis that the gene expression of PBMCs changes in response to diabetic circumstances, we comprehensively compared global gene expression profiles of PBMCs between patients with and without type 2 diabetes and between patients with type 2 diabetes before and after glycemic control, by using DNA microarray technology. We extracted the metabolic pathways coordinately altered in the PBMCs of patients with type 2 diabetes and identified the c-Jun N-terminal kinase (JNK) and OXPHOS pathways as surrogate transcriptional markers for hyperglycemia-induced oxidative stress and morbidity of type 2 diabetes, respectively. This finding may lead to the novel and powerful application of gene expression profile analysis of PBMCs for exploring the pathophysiology of diabetes.

Materials and methods

Patients. Eighteen patients with type 2 diabetes admitted to Kanazawa University Hospital between 2002 and 2004 and sixteen non-diabetic subjects were enrolled in this study. The clinical characteristics of the study subjects are shown in Table 1. No subjects had chronic inflammatory diseases such as collagen diseases and infectious diseases, all tested negative for the hepatitis B and C viruses, and all reported drinking less than 20 g/day of ethanol. The patients were diagnosed based on criteria established by an expert committee on the diagnosis and classification of diabetes mellitus [10]. The patients with diabetes were treated with diet therapy alone, oral hypoglycemic agents, or insulin as described in Table 1. Some patients were prescribed with agents for hypertension and dyslipidemia such as statins, angiotensin-converting enzyme inhibitors, or angiotensin II receptor type 1 blockers (Table 1). Overweight subjects were defined as those with a body mass index (BMI) $\geqslant 25\ kg/m^2$, which is the Japanese criteria of obesity [11].

All patients were treated for hyperglycemia at our outpatient clinic for 328 ± 235 days, and their blood samples were analyzed before and after glycemic control (Table 1).

All patients provided written informed consent for this study. The experimental protocol was approved by the relevant ethics committee of our institution and was carried out in accordance with the Declaration of Helsinki.

Laboratory studies. After an overnight fast, venous blood samples were withdrawn from each patient. Serum samples were assayed for plasma glucose, HbA_{1C}, total cholesterol, triglycerides, HDL cholesterol, insulin, alanine aminotransferase, aspartate aminotransferase (AST), hs-CRP, free fatty acids, and adipocytokines such as adiponectin, leptin, and tumor necrosis factor-α (TNF-α).

Isolation of RNA from PBMCs and amplification of antisense RNA. Heparinized blood samples were withdrawn from the peripheral vessels of subjects, and mononuclear cells were isolated by the Ficoll density-gradient method as previously described [12]. Total RNA was isolated from PBMC samples by using a Micro RNA isolation kit (Stratagene, La Jolla, CA) and RNeasy mini column (QIAGEN, Chatsworth, CA). Antisense RNA was synthesized and amplified using 2 μg of the isolated RNA with an Amino Allyl MessageAmp aRNA kit (Ambion, Austin, TX).

Preparation of fluorescently labelled cDNA and microarray hybridization. To label the probes, approximately 5 μg of amplified aRNA was chemically coupled to Cy3 or CY5 mono-reactive dye (Amersham) in accordance with the manufacturer's protocol. As a reference for each hybridization, we used aRNA samples prepared from the PBMCs of a 29-year-old healthy man. Reference aRNAs were labelled with Cy3, and test sample aRNAs were labelled with Cy5. Hybridization experiments were as described (http://www.dna-chip.co.jp/thesis/AceGeneProtocol.pdf). Briefly, the labelled probes were purified on Microcon 30 columns (Millipore, Bedford, MA); each mixture was concentrated to 31 μL. After fragmentation, 25 μL of 5× standard saline citrate (SSC), 5 μL of 10% sodium dodecyl sulphate, 8 μL of 50× Denhardt's solution, 1 μL of salmon sperm DNA (10 μg/μL), 20 μL of 5 M tetramethyl ammonium chloride, and 10 μL of formamide were added. Each 100-μL aliquot was used as a hybridization probe for the oligo-DNA chip (AceGene®Human Oligo Chip 30 K, HitachiSoft, Japan). The slides were covered with glass coverslips, fixed in a hybridization cassette (TeleChem, Sunnyvale, CA), and hybridized at 65 °C for 16 h. The slides were washed in 2× SSC and 0.03% sodium dodecyl sulphate for 5 min, 1× SSC for 5 min, and 0.2× SSC for 5 min.

Image analysis. The fluorescence intensity of each spot on the hybridized oligo-DNA microarray plate was obtained with a DNA microarray scan array G (Perkin-Elmer, Wellesley, MA). The images were quantified by DNASIS array v. 2.6 software (Hitachi Software Engineering Co., Ltd., Yokohama, Japan). The signal intensity of each spot was calibrated by subtracting adjacent background signals. To normalize the data, we averaged the intensities of all spots obtained with Cy3 and Cy5 in each of the 16 rectangles and adjusted the intensity of each corrected DNA spot by the average intensity ratio Cy5/Cy3 = 1.0. This global normalization of intensity provided a smaller variance of the Cy5/Cy3 ratio and almost equivalent results as normalization using housekeeping genes.

Hierarchical clustering of the gene expression in the patients was assessed by calculating Pearson's product-moment correlation coefficient using BRB-Array Tools software (NCBI, NIH, USA) [13]. The data were log transformed, normalized, mean centered, and applied to the average linkage clustering. The resulting dendrogram indicated the order in which patients were grouped based on the similarities of their gene expression patterns. The gene cluster data are presented graphically, and the analyzed genes are arranged as ordered by the clustering algorithm, so that genes with the most similar expression patterns are placed adjacent to each other.

Statistical analysis. All data are expressed as means ± SEM. To test the significance of expression ratios of individual genes or pathways, we used supervised analyses with a permutation-based method by using the BRB-Array Tools software [13]. This is the Class Comparison Tool based on univariate *F*-tests to find genes differentially expressed between predefined clinical groups. The permutation distribution of the *F*-statistic, based on 2000 random permutations, was also used to confirm statistical significance. We screened a total of 535 human gene sets, which included 285 BioCarta pathways, 101 KEGG pathways, and 149 gene sets previously described [14].

We normalized the expression levels of the 48 genes involved in the JNK pathway and 92 genes involved in the OXPHOS pathway to a mean of 0 and a variance of 1 across all samples. The mean centroid is the mean of the normalized gene expression levels [4,14]. A P value of <0.005 was considered significant.

Results

Patients characteristics

Clinical characteristics of the study subjects and the patients with diabetes before and after glycemic control

Table 1
Clinical characteristics of the patients with type 2 diabetes (T2DM) before (pre) and after (post) glycemic control

	Non-DM	T2DM	
		Pre	Post
No. (M:F)	16 (14:2)	18 (10:8)	18 (10:8)
Age (years)	26 ± 2	55 ± 17*	(after 328 ± 235 days)
BMI (kg/m^2)	21.1 ± 1.9	26.0 ± 5.4*	27 ± 5.1
Fasting plasma glucose (mmol/l)	4.6 ± 0.7	16.2 ± 15.4*	7.28 ± 2.11**
HbA_{1C} (%)	ND	11.0 ± 2.7	6.8 ± 1.5**
Total cholesterol (mmol/l)	4.62 ± 0.72	5.07 ± 0.85	5.04 ± 1.13
Triglyceride (mmol/l)	1.17 ± 0.60	1.80 ± 2.09	1.17 ± 0.65
HDL-cholesterol (mmol/l)	1.55 ± 0.31	1.34 ± 0.31	1.37 ± 0.31
Alanine aminotransferase (IU/l)	14 ± 8	35 ± 23 *	28 ± 15
hs-CRP (μg/dl)	0.070 ± 0.093	0.097 ± 0.088	0.13 ± 0.15
Tumor necrosis factor-α (pg/ml)	1.1 ± 0.65	1.3 ± 0.31	1.6 ± 0.53
Adiponectin (μg/ml)	8.5 ± 2.2	8.0 ± 4.7	11 ± 9
Leptin (ng/ml)	0.65 ± 0.31	12.6 ± 13.1 *	8.5 ± 2.2
Free fatty acids (mEq/L)	0.65 ± 0.31	1.0 ± 0.38*	0.94 ± 0.38
Treatments for diabetes			
Diet therapy alone		7	2
Metformin		2	1
Pioglitazone		2	2
Sulphonylureas		6	3
Insulin		5	11
Treatments for hypertension and hyperlipidaemia			
ACE-I or ARB		2	3
Statins		6	5

ACE-I, Angiotensin converting enzyme inhibitor; ARB, Angiotensin receptor type I blocker; Non-DM, Non-diabetic subjects; T2DM, Patients with type 2 diabetes. Data are expressed as means ± SD.
* $P < 0.05$ vs. Non-DM.
** $P < 0.05$ vs. Pre.

are shown in Table 1. Age, BMI, and levels of fasting plasma glucose, HbA_{1c}, alanine aminotransferase, leptin and free fatty acids were significantly increased in patients with type 2 diabetes. There were no significant differences in levels of adiponectin and inflammatory markers such as hs-CRP and TNF-α between diabetic and non-diabetic subjects (Table 1). The patients with diabetes were treated mainly with insulin and improved in glycemic control as described in Table 1. The use of drugs that may affect the gene expression in the PBMCs such as metformin, pioglitazone, angiotensin converting enzyme inhibitor, angiotensin receptor type I blocker or statins were not changed in most patients between before and after glycemic control. There were no significant differences in levels of inflammatory markers and adipocytokines between before and after glycemic control (Table 1).

Differential gene expression in PBMCs obtained from patients with type 2 diabetes mellitus

To explore whether the gene expression in PBMCs obtained from patients with type 2 diabetes differs from that of non-diabetic subjects, we applied supervised and non-supervised learning methods to classify the gene expression profiling. With a hierarchical clustering analysis, a non-supervised learning method, using 29,597 non-filtered genes, the patients were roughly clustered into three groups: patients with diabetes before glycemic control, patients with diabetes after glycemic control, and non-diabetic subjects.

Supervised learning methods based on the compound covariate predictor revealed that, among the various clinical parameters, only two clinical parameters, glycemic control and the presence of diabetes, significantly classified these patients (Supplementary Table 1). In contrast, age, gender, and BMI were not clinical determinants of gene expression profiling (data not shown).

Pathways that determine diabetes and the glycemic level

To examine which signalling pathways were evoked in PBMCs in type 2 diabetes, we compared the gene expression profiles obtained from type 2 diabetes patients and non-diabetic subjects. Moreover, we compared the gene expression in PBMCs obtained from pre-treated and post-treated patients with type 2 diabetes to explore which signalling pathway could be rescued by the treatment of type 2 diabetes. We screened a total of 535 human pathways determined by BioCarta, the KEGG pathway, and Affymetrix (http://www.affymetrix.com) and extracted the metabolic pathways that were significantly altered in the PBMCs of the subject groups (Table 2, Supplementary Table 2). Various pathways such as the OXPHOS (VOXPHOS_h), MAPK (ST_JNK_MAPK_Pathway_h), and electron transport chain pathways were significantly altered between subjects with and without diabetes (Table

2, Supplementary Table 2). On the other hand, pathways involved in the stress response, such as the MAPK, TNF signalling, apoptosis, and mTOR signalling pathways, were significantly altered after glycemic control (Table 2, Supplementary Table 2). These pathways were not significantly altered by age, gender, or BMI in the PBMCs of the patients with diabetes (data not shown).

The JNK pathway reflects hyperglycemia

The only pathway genes coordinately altered commonly by the existence of diabetes (pre-treated diabetic patients vs. non-diabetic subjects) and by glycemic control (pre-treated vs. post-treated diabetic patients), but not altered between post-treated diabetic patients and non-diabetic subjects, were the 48 genes involved in the JNK pathway (Table 2, Supplementary Table 3). With respect to individual genes, 10 of 48 genes involved in the JNK pathway were significantly up-regulated ($P < 0.05$), and 14 of 48 genes were significantly down-regulated after glycemic control ($P < 0.05$).

To further address the significance of the JNK pathway in the pathophysiology of type 2 diabetes, we computed the mean centroid of the JNK genes as previously described [4,14]. The JNK mean centroid was significantly higher in patients with diabetes compared with non-diabetic subjects and was significantly decreased after glycemic control (Fig. 1A).

We next evaluated the correlation of the expression level of JNK genes in the PBMCs and clinical or biochemical parameters of individuals with type 2 diabetes (Table 3). The JNK mean centroid in the PBMCs was significantly correlated with levels of fasting plasma glucose and A1C. Thus, the up-regulation of the JNK genes in the PBMCs may be associated with hyperglycemia.

OXPHOS pathway reflects morbidity of type 2 diabetes

The only pathway genes coordinately altered by the existence of diabetes (pre-treated diabetic patients vs. non-diabetic subjects and post-treated diabetic patients vs. non-diabetic subjects), but not altered by glycemic control (pre-treated vs. post-treated diabetic patients), were the 92 genes involved in the mitochondrial OXPHOS pathway and 96 genes involved in the electron transport chain pathway, which share most of the same genes (Table 2, Supplementary Table 4). With respect to individual genes, 30 of 92 genes involved in the OXPHOS pathway were significantly down-regulated, and no genes were significantly up-regulated in diabetes ($P < 0.05$).

The OXPHOS mean centroid was significantly down-regulated in patients with diabetes compared with non-diabetic subjects, whereas it was not significantly altered after glycemic control (Fig. 1B).

As shown in Table 3, the OXPHOS mean centroid in the PBMCs did not significantly correlate with the fasting levels of plasma glucose and HbA_{1C}. Thus, the down-regulation of OXPHOS genes may be determined genetically and may reflect the morbidity of type 2 diabetes.

Discussion

In the present study, we demonstrated the possibility that gene expression profiles in PBMCs reflect the pathophysiology of type 2 diabetes. As type 2 diabetes is a multifactorial disorder [15], a comprehensive approach

Table 2
Significantly altered pathways in diabetic PBMC

	Pathway description	No. of genes	T2DM-Pre vs. Non-DM		T2DM-Post vs. T2DM-Pre	
			LS permutation *p*	KS permutation *p*	LS permutation *p*	KS permutation *p*
1	Electron_Transport_Chain_h	96	0.0000905	0.0087215	0.3297651	0.1435376
2	VOXPHOS_h	92	0.0009636	0.0269323	0.2323794	0.0899932
3	HOXA9_DOWN_h	42	0.011004	0.0045108	0.0643224	0.2061987
4	4fcer1 Pathway_h	44	0.01321	0.0186952	0.4412977	0.4359556
5	pparaPathway_h	62	0.0165551	0.1204174	0.6542218	0.7514925
6	MAP00620_Pyruvate_metabolism_h	40	0.0169308	0.0955992	0.6148643	0.6883807
7	p38mapkPathway_h	55	0.0278384	0.0945286	0.0759194	0.184746
8	CR_IMMUNE_FUNCTION_h	57	0.0298111	0.0008373	0.5589565	0.8259213
9	keratinocytePathway_h	53	0.0298347	0.0827755	0.2315696	0.316895
10	ST_Fas_Signaling_Pathway_h	81	0.0309935	0.1369283	0.1961165	0.053945
11	metPathway_h	47	0.0314289	0.2487016	0.2889148	0.1813162
12	CBF_LEUKEMIA_DOWNING_AML_h	81	0.0356794	0.3177211	0.0464059	0.0042596
13	ST_B_Cell_Antigen_Receptor_h	48	0.0370735	0.2309135	0.1514077	0.2013602
14	ST_JNK_MAPK_Pathway_h	48	0.0463635	0.0181573	0.0082456	0.0048617
15	erkPathway_h	40	0.0473747	0.0488313	0.1155434	0.0388996
16	INSULIN_2F_DOWN_h	40	0.0529183	0.0283123	0.0496545	0.0783795
17	MAP00071_Fatty_acid_metabolism_h	46	0.0548243	0.0433901	0.9451761	0.9641461
18	bcrPathway_h	42	0.066755	0.3680323	0.5129712	0.678769
19	MAP00561_Glycerolipid_metabolism_h	54	0.0672738	0.0125806	0.9263149	0.9473428
20	integrinPathway_h	45	0.0748778	0.4564322	0.0871219	0.1522387

Non-DM, Non-diabetic subjects; Post, After glycemic control; Pre, Before glycemic control; T2DM, Patients with type 2 diabetes.

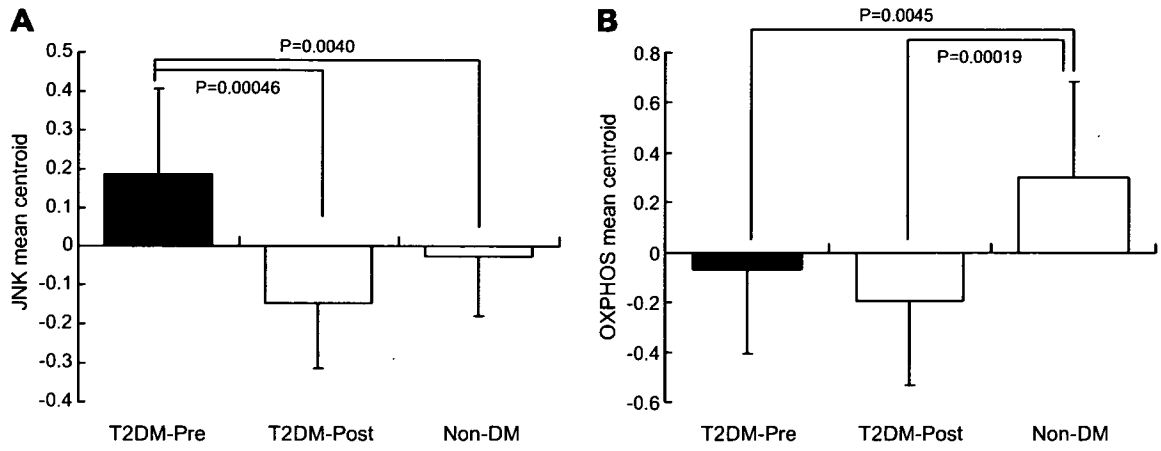

Fig. 1. JNK mean centroid (A) and OXPHOS mean centroid (B) in patients with type 2 diabetes (T2DM) before (Pre) and after (Post) glycemic control and in non-diabetic subjects (Non-DM). The mean centroid of the OXPHOS genes was computed as described in Methods. The values are means ± SD.

Table 3
Correlation of mean centroid of the genes involved in pathways for OXPHOS and JNK with the clinical parameters in patients with type 2 diabetes

	JNK mean centroid		OXPHOS mean centroid	
	Pearson's r	P	Pearson's r	P
BMI	0.018	0.920	−0.252	0.143
Fasting plasma glucose	0.468	0.018	0.097	0.644
HbA_{1C}	0.393	0.022	0.169	0.338
Fasting insulin	0.528	0.360	0.739	0.153
Alanine aminotransferase	0.232	0.208	0.127	0.496
Total cholesterol	0.154	0.417	−0.024	0.900
Triglyceride	0.098	0.606	0.093	0.624
HDL-cholesterol	0.030	0.874	0.120	0.527
hs-CRP	−0.068	0.789	−0.333	0.177
TNF-α	−0.355	0.125	−0.287	0.219
Adiponectin	−0.184	0.411	0.281	0.205
Leptin	−0.215	0.336	−0.166	0.459
Free fatty acids	0.255	0.291	0.302	0.209

identifying biological pathways or co-regulated gene sets associated with the diseases should be required to understand the molecular signature of type 2 diabetes [4]. Thus, we screened known human pathways and extracted the metabolic pathways that were significantly altered in the PBMCs of the subject groups.

We found that the distinct pathophysiology of patients with type 2 diabetes was reflected by coordinate alterations in the gene expression levels of the JNK and mitochondrial OXPHOS pathways in PBMCs; the former reflected hyperglycemia-associated oxidative stress, and the latter reflected an intrinsic alteration in patients with type 2 diabetes.

It has been recognized that, in endothelial cells, hyperglycemia causes mitochondrial superoxide production that leads to oxidative stress via glucose-induced activation of protein kinase C, increased formation of glucose-derived advanced glycation end-products, and increased glucose flux through the aldose reductase pathway [2]. Such diabetes- or hyperglycemia-induced oxidative stress may cause endoplasmic reticulum stress leading to activation of the JNK pathway in pancreatic beta-cells and hepatocytes [16]. The activation of JNK suppresses insulin biosynthesis and interferes with insulin action. Indeed, the suppression of JNK in diabetic mice was found to improve insulin resistance and ameliorate glucose tolerance [16]. Thus, the JNK pathway plays a central role in the pathogenesis of type 2 diabetes and could be a potential target for diabetes therapy. This glucose-induced oxidative stress can occur systemically, especially in PBMCs that uptake glucose in an insulin-independent manner. In the present study, the genes involved in the JNK pathway of the PBMCs were coordinately up-regulated in diabetes and significantly down-regulated after glycemic control, whereas the inflammatory markers (hs-CRP and TNF-α) and adipocytokines (adiponectin and leptin) were not altered. Thus, it might be possible that we can estimate the glucose-induced oxidative stress in pancreatic beta cells, hepatocytes, and endothelial cells simply by analyzing the gene expression profile in the PBMCs of patients with type 2 diabetes.

On the other hand, the OXPHOS pathway may predict the existence of diabetes because it was coordinately down-regulated in the PBMCs of patients with type 2 diabetes,

but was not altered by glycemic control. Emerging evidence supports the potentially unifying hypothesis that insulin secretory failure and insulin resistance, both of which are prominent features of type 2 diabetes, are caused by mitochondrial dysfunction [17]. Indeed, type 2 diabetes is associated with the coordinate down-regulation of genes involved in OXPHOS in skeletal muscle [14] and adipose tissue [18]. This alteration might occur genetically and systemically in patients with type 2 diabetes, except in the liver in which excess metabolites of glucose and fatty acids may up-regulate the genes involved in OXPHOS [4]. Thus, it might be possible to predict the predisposition or onset of type 2 diabetes simply by analyzing the gene expression profile of PBMCs.

Although future studies are necessary to clarify the effects of age, gender, type of diabetes, complications, treatment regimens for diabetes, other pharmacological treatments for hypertension and hyperlipidemia, etc., the present study suggests the diagnostic potential of gene expression analysis of PBMCs in patients with type 2 diabetes.

Appendix A. Supplementary data

Supplementary data associated with this article can be found, in the online version, at doi:10.1016/j.bbrc.2007.07.006.

References

[1] C. de Luca, J.M. Olefsky, Stressed out about obesity and insulin resistance, Nat. Med. 12 (2006) 41–42.
[2] T. Nishikawa, D. Edelstein, X.L. Du, S. Yamagishi, T. Matsumura, Y. Kaneda, M.A. Yorek, D. Beebe, P.J. Oates, H.P. Hammes, I. Giardino, M. Brownlee, Normalizing mitochondrial superoxide production blocks three pathways of hyperglycaemic damage, Nature 404 (2000) 787–790.
[3] T. Takamura, M. Sakurai, T. Ota, H. Ando, M. Honda, S. Kaneko, Genes for systemic vascular complications are differentially expressed in the livers of Type 2 diabetic patients, Diabetologia (2004).
[4] H. Misu, T. Takamura, N. Matsuzawa, A. Shimizu, T. Ota, M. Sakurai, H. Ando, K. Arai, T. Yamashita, M. Honda, T. Yamashita, S. Kaneko, Genes involved in oxidative phosphorylation are coordinately upregulated with fasting hyperglycaemia in livers of patients with type 2 diabetes, Diabetologia 50 (2007) 268–277.
[5] Y. Tahara, K. Shima, Kinetics of HbA1c, glycated albumin, and fructosamine and analysis of their weight functions against preceding plasma glucose level, Diabetes Care 18 (1995) 440–447.
[6] The relationship of glycemic exposure (HbA1c) to the risk of development and progression of retinopathy in the diabetes control and complications trial, Diabetes 44 (1995) 968–983.
[7] H.C. Gerstein, J.F. Mann, Q. Yi, B. Zinman, S.F. Dinneen, B. Hoogwerf, J.P. Halle, J. Young, A. Rashkow, C. Joyce, S. Nawaz, S. Yusuf, Albuminuria and risk of cardiovascular events, death, and heart failure in diabetic and nondiabetic individuals, Jama 286 (2001) 421–426.
[8] A.I. Adler, R.J. Stevens, S.E. Manley, R.W. Bilous, C.A. Cull, R.R. Holman, Development and progression of nephropathy in type 2 diabetes: the United Kingdom Prospective Diabetes Study (UKPDS 64), Kidney Int. 63 (2003) 225–232.
[9] J.K. Pai, T. Pischon, J. Ma, J.E. Manson, S.E. Hankinson, K. Joshipura, G.C. Curhan, N. Rifai, C.C. Cannuscio, M.J. Stampfer, E.B. Rimm, Inflammatory markers and the risk of coronary heart disease in men and women, N. Engl. J. Med. 351 (2004) 2599–2610.
[10] Expert committee on the diagnosis and classification of diabetes mellitus, Report of the expert committee on the diagnosis and classification of diabetes mellitus, Diabetes Care 26 Suppl. 1 (2003) S5-20.
[11] T. Ota, T. Takamura, N. Hirai, K. Kobayashi, Preobesity in World Health Organization classification involves the metabolic syndrome in Japanese, Diabetes Care 25 (2002) 1252–1253.
[12] M. Tateno, M. Honda, T. Kawamura, H. Honda, S. Kaneko, Expression profiling of peripheral blood mononuclear cells from patients with chronic hepatitis C undergoing interferon therapy, J. Infect. Dis. 195 (2007) 255–267.
[13] Q.H. Ye, L.X. Qin, M. Forgues, P. He, J.W. Kim, A.C. Peng, R. Simon, Y. Li, A.I. Robles, Y. Chen, Z.C. Ma, Z.Q. Wu, S.L. Ye, Y.K. Liu, Z.Y. Tang, X.W. Wang, Predicting hepatitis B virus-positive metastatic hepatocellular carcinomas using gene expression profiling and supervised machine learning, Nat. Med. 9 (2003) 416–423.
[14] V.K. Mootha, C.M. Lindgren, K.F. Eriksson, A. Subramanian, S. Sihag, J. Lehar, P. Puigserver, E. Carlsson, M. Ridderstrale, E. Laurila, N. Houstis, M.J. Daly, N. Patterson, J.P. Mesirov, T.R. Golub, P. Tamayo, B. Spiegelman, E.S. Lander, J.N. Hirschhorn, D. Altshuler, L.C. Groop, PGC-1alpha-responsive genes involved in oxidative phosphorylation are coordinately downregulated in human diabetes, Nat. Genet. 34 (2003) 267–273.
[15] S. O'Rahilly, I. Barroso, N.J. Wareham, Genetic factors in type 2 diabetes: the end of the beginning? Science 307 (2005) 370–373.
[16] H. Kaneto, Y. Nakatani, D. Kawamori, T. Miyatsuka, T.A. Matsuoka, M. Matsuhisa, Y. Yamasaki, Role of oxidative stress, endoplasmic reticulum stress, and c-Jun N-terminal kinase in pancreatic beta-cell dysfunction and insulin resistance, Int. J. Biochem. Cell Biol. 37 (2005) 1595–1608.
[17] B.B. Lowell, G.I. Shulman, Mitochondrial dysfunction and type 2 diabetes, Science 307 (2005) 384–387.
[18] I. Dahlman, M. Forsgren, A. Sjogren, E.A. Nordstrom, M. Kaaman, E. Naslund, A. Attersand, P. Arner, Downregulation of electron transport chain genes in visceral adipose tissue in type 2 diabetes independent of obesity and possibly involving tumor necrosis factor-{alpha}, Diabetes 55 (2006) 1792–1799.

American Journal of Gastroenterology

Published by Blackwell Publishing

ISSN 0002-9270
doi: 10.1111/j.1572-0241.2007.01354.x

Impact of Diabetes on Recurrence of Hepatocellular Carcinoma after Surgical Treatment in Patients With Viral Hepatitis

Takuya Komura, M.D.,[1] Eishiro Mizukoshi, M.D.,[1] Yuki Kita, M.D.,[2] Masaru Sakurai, M.D.,[2] Yoshiko Takata, M.D.,[1] Kuniaki Arai, M.D.,[1] Tatsuya Yamashita, M.D.,[1] Tetsuo Ohta, M.D.,[3] Koichi Shimizu, M.D.,[3] Yasunari Nakamoto, M.D.,[1] Masao Honda, M.D.,[1] Toshinari Takamura, M.D.,[2] and Shuichi Kaneko, M.D.[1]

[1]*Department of Gastroenterology,* [2]*Department of Diabetes and Digestive Disease, and* [3]*Department of Gastroenterologic Surgery, Graduate School of Medicine, Kanazawa University, Kanazawa, Ishikawa, Japan*

OBJECTIVES: **Consensus has been reached that diabetes is a risk factor for development of HCC, but the impact on postoperative recurrence is still controversial. To clarify this point, we analyzed the relationship of postoperative recurrence rate of HCC and coexistence of diabetes in the patients with viral hepatitis.**

METHODS: **A total of 90 patients who had undergone curative resection for HCC were analyzed. They were divided into two groups with and without diabetes, and the recurrence-free survival rates after surgical treatment and the factors contributing to recurrence were examined.**

RESULTS: **Kaplan-Meier survival analysis showed the recurrence-free survival rates in the diabetic group were significantly lower than those in the nondiabetic group ($P = 0.005$) and overall survival rates in the diabetic group were significantly lower than those in the nondiabetic group ($P = 0.005$). These results were emphasized in the analysis of patients infected with hepatitis C virus. Univariate and multivariate analyses showed diabetes was a significant factor contributing to HCC recurrence after treatment. Furthermore, multivariate analysis in HCC patients with diabetes showed Child-Pugh classification B ($P = 0.001$) and insulin therapy ($P = 0.049$) were significant factors contributing to HCC recurrence after treatment.**

CONCLUSIONS: **The results of the present study suggest that diabetes is a risk factor for the recurrence of HCV-related HCC and decreases the overall survival rates after surgical treatment. HCV-related HCC patients with diabetes should be closely followed for postoperative recurrence.**

(Am J Gastroenterol 2007;102:1939–1946)

INTRODUCTION

Hepatocellular carcinoma (HCC) is the fifth most frequent malignant neoplasm in the world (1), and its prevalence is particularly high in Asia and Africa. The recent increase in its prevalence has attracted the attention of researchers (2, 3). Surgical therapy provides complete cure for HCC, but the indication is limited to a relatively small number of patients. Recent remarkable advances in diagnostic imaging techniques and systematic hepatectomy have been improving the prognosis of patients with HCC, but these techniques have not provided satisfactory results (4, 5), because of a high post-treatment recurrence rate characterizing HCC. Previous studies have noted that factors contributing to recurrence include gender, alcohol consumption, hepatitis C virus (HCV) infection, hepatic reserve, liver fibrosis degree, tumor size, tumor differentiation degree, vascular factor, and alpha-fetoprotein (AFP) level (6–9).

On the other hand, recent studies have reported that coexistence of diabetes is a risk factor for the progression of liver fibrosis and the development of HCC in chronic hepatitis C (10, 11). These reports suggest that coexistence of diabetes is also involved in the high postoperative recurrence rate of HCC. However, it is controversial whether diabetes is an independent risk factor for the post-treatment recurrence of HCC. Ikeda *et al.* (12) reported that diabetes was a risk factor for the recurrence of HCC after surgical treatment, but Poon *et al.* (13) and Toyoda *et al.* (14) reported that this was not the case. The discrepancy among these reports is probably due in part to the difference in the etiology of liver disease in the patients studied.

In this study, to clarify the controversial point about diabetes and HCC recurrence, we examined the impact of diabetes on the postoperative recurrence of HCC in 90 patients who had undergone curative resection for HCC. In addition, we classified the HCC patients into groups of hepatitis B

virus (HBV)- and HCV-related HCC patients, and performed a close analysis of the impact of diabetes on the postoperative recurrence of HCC in each group.

PATIENTS AND METHODS

Patients

A total of 150 patients were diagnosed with primary HCC and underwent surgical treatment in Kanazawa University Hospital between June 1987 and May 2004. Of these patients, 90 were analyzed who had HBV or HCV infection and underwent curative resection.

HCCs were detected by imaging modalities such as ultrasound scan, dynamic CT scan, MR imaging, and abdominal arteriography. The diagnosis of HCC was made by typical hypervascular tumor staining on angiography in addition to using typical findings, which showed hyperattenuation areas in the early phase and hypoattenuation in the late phase on dynamic CT (15).

All resected tumors were examined pathologically for the degree of differentiation of HCC, vascular invasion, and persistence of tumor in the surgical stump. Pathological degree of differentiation of HCC was assessed according to the general rules for the clinical and pathologic study of primary liver cancer (16).

Treatment and Follow-Up

In selecting surgery as a treatment option for HCC, we considered the following criteria: (a) good general condition of the patient whose Karnofsky performance status was over 80, (b) primary HCC, (c) Child-Pugh classification A or B, (d) the number of HCC was solitary and no CT, MRI, or angiographic evidence of vascular invasion or distant metastasis. Curative resection was defined as complete excision of the tumor with tumor-free surgical margins and no local recurrence at the surgical margin within 6 months after surgery.

Patients were followed postoperatively on an outpatient basis by abdominal ultrasound, dynamic CT, or MRI at 3-month intervals for at least 60 months. Recurrence was diagnosed by dynamic CT or MRI, and the date of recurrence was defined as the date of examination when the recurrence of HCC was noted. In patients with recurrent HCC, the recurrence-free period was defined as the time between the date of surgery and the date of recurrence. We confirmed the date of the patient's last visit to our hospital and checked the status of HCC using each patient's medical record.

Laboratory and Virologic Testing

Blood samples were tested for hepatitis B surface antigen (HBs-Ag) and hepatitis C virus antibody (HCV-Ab) by commercial immunoassays (Fuji Rebio, Tokyo, Japan). Serum AFP level was measured by enzyme immunoassay (AxSYM AFP, Abbott Japan, Tokyo, Japan). Diabetes was diagnosed according to the American Diabetes Association criteria for type II diabetes (17) and the severity of liver disease (stage of fibrosis) was evaluated according to the criteria of Desmet *et al.* (18).

Statistical Analysis

Between-group differences were assessed by univariate analysis with Student's *t*-test for numerical data and the $\chi 2$ test with Yates' correction (or Fisher's exact test where appropriate) for nominal data. Overall survival and recurrence-free survival was examined using the method of Kaplan-Meier, and differences were assessed by the log-rank test. Impact factors for the recurrence of HCC after hepatic resection were analyzed by univariate and multivariate analysis using Cox proportional hazards model. Seventeen variables were analyzed, consisting of age, gender, etiology, body mass index (BMI), prevalence of alcohol abuse, diabetes, hemoglobin A1c (HbA1c), liver fibrosis degree, Child-Pugh classification, platelet count, alanine aminotranseferase (ALT), T-bil, Alb, AFP, tumor size, tumor differentiation degree, and the presence of vascular invasion. $P < 0.05$ was considered statistically significant.

RESULTS

Comparison of Baseline Characteristics

Of the 90 patients (75 men and 15 women, with a mean age of 61.0 yr) who were followed and analyzed, 30 were diagnosed as having coexistence of diabetes, and 60 had no diabetes. The characteristics of the patients in both groups

Table 1. Characteristics of Patients

Characteristic	Patients With Diabetes (N = 30)	Patients Without Diabetes (N = 60)	*P* Value
Median age (yr)	62.0	60.6	0.453
Gender (male/female)	24/6	51/9	0.560
Etiology (HBV/HCV/ HBV + HCV)	8/22/0	17/40/3	0.438
Body mass index (kg/m^2)	23.5	22.73	0.316
Alcohol abuse (+/−)	13/17	27/33	0.881
HbA1c (%)	6.4	4.8	<0.001
HOMA-IR	4.1	3.3	0.399
Platelet count (× 10^4/μL)	12.2	13.5	0.284
ALT (IU/L)	69.8	56.4	0.318
Total bilirubin (mg/dL)	0.9	0.8	0.510
Albumin (g/dL)	4.1	4.2	0.341
AFP (ng/mL)	417	395	0.931
Fibrosis (F1/F2/F3/F4)	0/4/4/22	4/5/5/46	0.732
Inflammatory grading (A1/A2/A3)	11/17/2	24/33/3	0.385
Child-Pugh grade (A/B/C)	24/6/0	53/7/0	0.294
Tumor size (mm)	34.3	29.8	0.359
Diff. degree (wel/mod/por)*	11/12/7	20/19/21	0.264
Vascular invasion (+/−)	11/19	20/40	0.757
Date of operation (1987–1995/1995–2000/ 2001–2004)	8/14/8	13/30/17	0.538

*Histological degree of HCC: wel = well differentiated; mod = moderately differentiated; por = poorly differentiated.

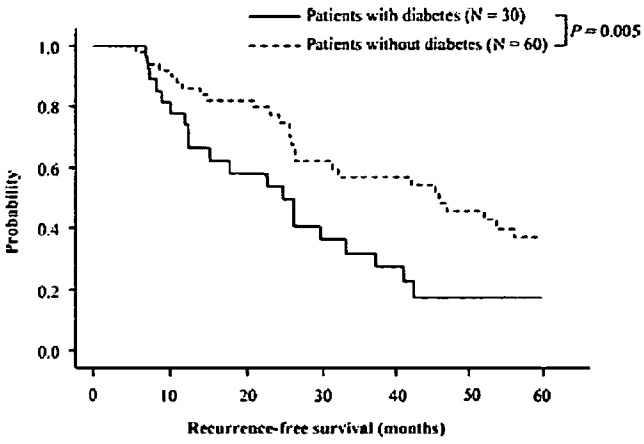

Figure 1. Kaplan-Meier curves for recurrence-free survival in the groups of patients with and without diabetes.

are shown in Table 1. No significant differences were noted between the two groups in age, gender, HBV or HCV infection rate, BMI, or prevalence of alcohol abuse. HbA1c was significantly higher, at 6.4%, in the diabetic group than in the nondiabetic group with an HbA1c of 4.8% ($P < 0.001$). There were no significant differences in platelet count, ALT, T-bil, Alb, AFP, or Child-Pugh classification between the two groups. In addition, no significant differences were observed in the liver fibrosis degree, or in the size, degree of differentiation, and presence of microscopic vascular invasion of resected HCC. Homeostasis model assessment-insulin resistance (HOMA-IR) of the patients with diabetes, which was high compared with that of Japanese healthy subjects (19), was higher than that of the patients without diabetes, although it was not statistically significant.

Impact of Diabetes on Recurrence After Surgical Treatment of HCC

Next, the diabetic and nondiabetic groups were compared for the rate of HCC recurrence after surgical treatment. HCC recurred after surgical treatment in 49 patients, consisting of 22 diabetic patients (73.3%) and 27 nondiabetic patients (45.0%). The mean time to recurrence was 32.8 months (range 8–60 months) and the median time to recurrence was 29.4 months.

Figure 1 shows the Kaplan-Meier curves for recurrence-free survival of the patients with and without diabetes. The recurrence-free survival rates 1, 2, 3, 4, and 5 yr after surgical treatment were 77.8%, 55.6%, 36.0%, 16.7%, and 16.7%, respectively, in the diabetic patient group, and 89.5%, 80.4%, 56.8%, 45.0%, and 36.6%, respectively, in the nondiabetic patient group; all rates except 1 yr were significantly lower in the diabetic patient group ($P = 0.155$, $P = 0.010$, $P = 0.009$, $P = 0.002$, and $P = 0.005$).

To further examine the degree of contribution of diabetes to the postoperative recurrence of HCC, we performed univariate and multivariate analysis. Univariate analysis identified the following variables as factors significantly contributing to HCC recurrence after surgical treatment: presence of diabetes ($P = 0.003$), high HbA1c level ($P < 0.001$), and Child-Pugh classification B against A ($P < 0.001$) (Table 2). When we conducted multivariate analysis, we chose variables that had already pointed out a risk factor for HCC recurrence and the P value was lower than 0.1 in univariate analysis. As a result, multivariate analysis of these variables showed that the presence of diabetes (risk 2.9, 95% CI 1.5–5.4, $P < 0.001$) and Child-Pugh classification B against A (risk 3.6, 95% CI 1.7–7.7, $P = 0.001$) were significant factors contributing to HCC recurrence after surgical treatment (Table 3).

Table 2. Univariate Proportional Hazard Model for Recurrence of HCC After Surgical Treatment

Variable	Hazard Ratio	95% CI	P Value
Age (yr)	1.0	1.0–1.1	0.258
Gender (male)	0.5	0.3–1.1	0.104
Etiology (HCV)	1.0	0.5–1.8	0.965
Body mass index (>25 kg/m^2)	1.2	0.6–2.3	0.554
Alcohol abuse (+)	1.1	0.7–2.0	0.644
Diabetes (+)	2.4	1.3–4.2	0.003
HbA1c (%)	1.5	1.2–1.9	<0.001
Fibrosis (F4)	1.4	0.7–3.1	0.349
Child-Pugh grade (B)	3.1	1.6–6.0	<0.001
Platelet count ($\times 10^4/\mu$L)	1.0	0.9–1.0	0.465
ALT (IU/L)	1.0	1.0–1.1	0.717
Total bilirubin (mg/dL)	1.4	0.6–3.6	0.451
Albumin (g/dL)	1.4	0.8–2.4	0.225
AFP (>200 ng/mL)	1.0	0.5–1.8	0.906
Tumor size (>50 mm)	1.5	0.7–1.2	0.213
Diff. degree (P)	1.1	0.6–2.1	0.675
Vascular invasion (+)	1.2	0.4–1.7	0.490

Impact of Diabetes on Prognosis After Surgical Treatment of HCC

To examine the impact of diabetes on prognosis of HCC patients, we analyzed the overall survival rates after surgical treatment. Figure 2 shows the Kaplan-Meier curves for overall survival of the patients with and without diabetes after surgical treatment of HCC. The overall survival rates 1, 2, 3, 4, and 5 yr after surgical treatment were 100%, 88.9%, 75.0%, 63.6%, and 45.5%, respectively, in the diabetic patient group, and 100%, 98.1%, 88.9%, 85.7%, and 76.3%, respectively, in the nondiabetic patient group; the rates of more than 3 yr were significantly lower in the diabetic patient group ($P = 1.000$, $P = 0.073$, $P = 0.028$, $P = 0.039$, and $P = 0.005$).

Table 3. Multivariate Proportional Hazard Model for Recurrence of HCC After Surgical Treatment

Variable	Hazard Ratio	95% CI	P Value
Diabetes	2.9	1.5–5.5	<0.001
Fibrosis (F4)	1.9	0.8–4.5	0.148
Child-Pugh grade (B)	3.6	1.7–7.7	0.001
AFP(>200 ng/mL)	0.7	0.3–1.5	0.390
Diff. degree (P)	0.9	0.5–1.8	0.776
Vascular invasion (+)	2.0	1.0–4.0	0.061